

1 **An Admissible Annual Load framework for nutrients in hypertrophic coastal**
2 **Mediterranean lagoons: a case study**

3 Annie Fiandrino^{a*}, Romain Pete^b, Dominique Munaron^c, Pierre Théliér^d, Valérie Derolez^c,
4 Lucille Picard^d, Olivier Boutron^e, Columba Martinez-Espinosa^e, Anaïs Giraud^f, Stéphane
5 Stroffek^g, Eve Le Pommelet^d, Vincent Ouisse^c.

6 ^a MARBEC, Univ Montpellier, CNRS, Ifremer, IRD, F-83507 La Seyne-sur-Mer, France

7 ^b Syndicat mixte du bassin de Thau, F-34200 Sète, France

8 ^c MARBEC, Univ Montpellier, CNRS, Ifremer, IRD, F-34203 Sète, France

9 ^d Syndicat mixte du Bassin de l'Or (Symbo), F-34400 Lunel, France

10 ^e Tour du Valat Research Institute, Le Sambuc, 13200 Arles, France

11 ^f Agence de l'eau Rhône Méditerranée Corse / Délégation de Montpellier, F-34961 Montpellier,
12 France

13 ^g Agence de l'eau Rhône Méditerranée Corse / Département de la Connaissance et de la
14 Planification, F-69363 Lyon, France

15 *Corresponding author: Annie Fiandrino (MARBEC, Ifremer, Zone Portuaire de Brégaillon,
16 CS20 330, F-83507 La Seyne-sur-Mer cedex, France)

17 *E-mail address: annie.fiandrino@ifremer.fr*

18 *For the purpose of Open Access, a CC-BY public copyright licence has been applied by the*
19 *authors to the present document and will be applied to all subsequent versions up to the Author*
20 *Accepted Manuscript arising from this submission.*

21 *Distributed under a Creative Commons Attribution | 4.0 International licence*



22 **Keywords:**

23 hypereutrophic coastal lagoon, box model, management tool, ecological restoration, pressure–
24 state chart

25 **Figures** : all figures of this manuscript need colors (except Fig.2,3 and 4)

26

27 **Abstract:**

28 The GAMELag box-model tool is used in a collaborative approach between scientists and
29 ecosystem managers to determine admissible nutrient load in lagoon environments. This case
30 study of its application in a hypereutrophic French Mediterranean lagoon demonstrated its
31 ability to determine exogenous nutrient flows compatible with good ecological status. A new
32 method, based on the exploratory analysis of simulated scenarios of flow reduction (exogenous
33 and endogenous), revealed the predominant role of sediment stocks and exchanges in the
34 ecological status of this lagoon. Reducing inflows from the catchment area allowed sediment
35 release and initiated the restoration of this compartment. A reduction in exogenous nitrogen
36 inputs by a factor of 0.24 and phosphorus by 0.1 was found to be necessary to achieve EU Water
37 Framework Directive objectives. These results are helping lagoon managers to raise the
38 awareness of local stakeholders and co-construct management measures to encourage a
39 dynamic of restoration.

40 **1. Introduction**

1.1 Context

41 An increase in nitrogen and phosphorus inflows from catchment areas with growing populations
42 and expanding anthropogenic activities, particularly since the 1960s, is recognised as a major
43 cause of the environmental degradation of coastal ecosystems (Cloern, 2001). On a global scale,
44 coastal lagoons are especially affected by the resulting eutrophication, which leads to profound
45 changes in the structure and functioning of these ecosystems and the services they provide
46 (Zaldívar et al., 2008; Pérez-Ruzafa et al., 2019). In Europe, since the mid-2000s, the EU Water
47 Framework Directive has required member states to restore the ecological quality of degraded
48 hydrosystems by implementing measures to reduce nutrient inputs and to monitor the
49 effectiveness of these management measures (Voulvoulis et al., 2017; de Wit et al., 2020;
50 Newton et al., 2022).

51 On the Mediterranean coast of France, following the application of the French Water Law (Law
52 no. 92-3 of 3 January 1992), which reinforced the powers of municipalities in water
53 management, the Rhône-Mediterranean-Corsica Water Agency (RMC Water Agency)
54 proposed that a network be set up to measure and monitor the quality of the basin's lagoons (in
55 the regions of Occitanie, Provence-Alpes-Côte d'Azur and Corsica) at the beginning of the
56 2000s. In parallel, the fishing and marine farming sectors expressed the need to develop
57 environmental management actions, as well as to receive regular information about the
58 environmental quality of waters on which their activities depend.

59 To this end, a partnership between public agencies and scientists led to the creation of the
60 Regional Lagoon Monitoring Network in 2002 with the twofold objective of (i) acquiring data
61 to diagnose the state of lagoons with regard to eutrophication, and (ii) developing tools to assess
62 the impact of nutrient inputs on the functioning of lagoon ecosystems and to assist in the
63 management of these environments. Since 2006, the monitoring programme required by the EU
64 Water Framework Directive (WFD) has been implemented in Mediterranean lagoons. The
65 Regional Lagoon Monitoring Network proved a solid base for WFD monitoring, since the
66 eutrophication indicators specific to lagoons measured by the network's protocol (Zaldívar et
67 al., 2008) were adopted and progressively consolidated to become WFD ecological status
68 indicators for these transitional water bodies. The resulting information about the degraded state
69 of almost all aquatic ecosystems in the region of Occitanie in France (Ifremer, 2003) has been
70 disseminated to the managers of lagoon environments, raising awareness and triggering, in line
71 with the WFD, the implementation of structural measures aimed at reducing urban waste
72 (Derolez et al., 2019).

73 Since 2009, in lagoons where efforts have been made to reduce pollutant loads, the restoration
74 process has raised questions about (i) the time required to restore all the ecosystem

75 compartments in a lagoon, and (ii) the maximum nitrogen and phosphorus loads compatible
76 with achieving and/or maintaining good ecological status.

77 The restoration of coastal environments involves either a direct return to a ‘pre-degradation’
78 state if disturbance levels are low (Greening et al., 2014), or more usually through a
79 phenomenon of hysteresis, i.e. a partial restoration with different and generally longer processes
80 than those occurring during degradation (Elliott et al., 2007; Duarte et al., 2009; Cloern et al.,
81 2020). This hysteresis is due to the complex functioning of the ecosystem, the presence of
82 threshold effects, and interconnected processes involving all the physical, chemical and
83 biological compartments that play a role in cycles of matter.

84 The time required to restore the most integrative compartments of the ecosystem is medium to
85 long (several years) (Borja et al., 2010), with the recolonisation of the environment by seagrass
86 beds taking up to ten years, as has been observed in Tampa Bay, Florida (USA) (Greening et
87 al., 2014). In lagoon environments, restoration time depends on: (i) the nutrient load from the
88 catchment area; (ii) the structure and functioning of the biological community (e.g. its role in
89 the matter cycle and storage of nutrients); (iii) exchanges between the benthic compartment and
90 the water column (particularly sediment release); and (iv) the capacity to export excess nitrogen
91 and phosphorus to the open environment (Ouisse et al., 2013; 2014).

92 1.2. ‘Admissible load’ approach

93 Maximum nutrient load is determined by the water planning and management regulations for
94 the Rhône-Mediterranean-Corsica basin, which defines the ‘admissible load’ for a lagoon as
95 “the maximum pollutant load in a catchment area that does not compromise its quality
96 standards. This corresponds to the maximum accumulation of a substance from discharge and
97 emissions of discrete or diffuse pollutants in a catchment area while maintaining compliance
98 with environmental quality criteria (ecological status, chemical status, specific objectives for
99 drinking water, shellfish farming, swimming, etc.)” (SDAGE, 2022).

100 More broadly, the ‘admissible load’ approach, which was developed to help managers tackle
101 the eutrophication of aquatic environments (SDAGE, 2018), aims to: (i) better identify and
102 quantify the various nutrient loads that reach a lagoon; (ii) estimate the admissible load of a
103 lagoon with regard to its capacity to receive this without permanently jeopardising its ecological
104 functioning; (iii) set an overall objective for reducing pollutant loads that is consistent with a
105 lagoon’s admissible load; (iv) define a restoration programme to implement relevant actions in
106 collaboration with all local stakeholders to reduce nutrient inputs to a targeted lagoon.

107 *1.3 A modelling approach to support lagoon management*

108 In this context, we aimed to build a robust and reliable tool to acquire knowledge on the
109 ecological functioning of eutrophicated lagoon ecosystems or those undergoing restoration
110 (Pete et al., 2020a). The resulting management tool, GAMELag (*Gestion et Aménagement des*
111 *Milieux Eutrophisés Lagunaires: Management of Eutrophic Lagoon Environments*), was
112 developed within the framework of the Regional Lagoon Monitoring Network and was guided
113 by the needs of managers responsible for restoring these ecosystems.

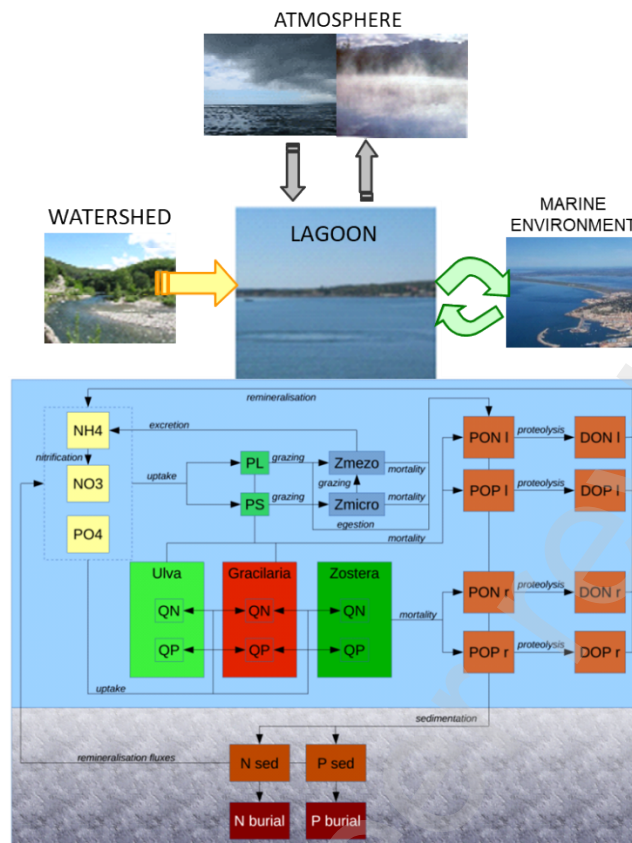
114 Modelling tools are relevant for addressing the issue of admissible load (Chapra et al., 2003).
115 Based on a review of more than 300 Total Maximum Daily Load (TMDL) approaches carried
116 out between 2015 and 2020 in the United States, Sridharan et al. (2021) found that those based
117 on process models that link cause and effect (1D or 2D) are preferable, yet are only used in 25%
118 of cases, with the large datasets required to implement these being their main limitation.

119 These authors also point out that the use of complex, high-resolution (3D) numerical models
120 cannot yet be envisaged for management applications because of the long calculation times
121 required. In this context, an alternative approach consists of using the results from high-
122 resolution models to produce data that cannot be measured in situ and/or new knowledge to
123 populate simpler management tools. In this way, the processes calculated in detail by powerful
124 but complex tools can be integrated into support tools in a relevant way. Such methods have

125 been used to develop tools to help assess the sanitary status of shellfish production areas
126 (Mongruel et al., 2013), as well as tools aimed at shellfish farmers so they can adapt their
127 farming practices and optimise their production in contexts of high interannual variability in
128 environmental quality or mortality (Cugier et al., 2022).

129 *1.4. A practical tool guided by management needs*

130 The GAMELag tool was developed following this same approach. This model is based on a
131 simplified representation of the ecosystem in ‘physical units’ (Gordon et al., 1996; Vijay et al.,
132 2021; Ferrarin et al., 2010) and ‘biological compartments’. A method based on the use of a
133 high-resolution hydrodynamic model makes it possible to define the necessary number of
134 physical units to account for the hydrodynamic functioning of a lagoon. The identification of
135 hydrodynamic boundaries and heterogeneous water masses within a lagoon conditions the
136 number of physical units to be considered (Fiandrino et al., 2017; Pete et al., 2017; 2020a).
137 Within each unit, the model simulates the temporal change in the quantities of nitrogen and
138 phosphorus stored in the main ecological compartments (water column, phytoplankton,
139 zooplankton, macrophytes, sediment) as a result of nutrient loads from the catchment area and
140 the atmosphere and exchanged (exported and imported) with the external marine environment
141 (Figure 1). In this way, the model makes the link between the biological status of a lagoon and
142 the pressures to which it is subjected.



143
 144 Figure 1: Conceptual diagram of the GAMELag model showing the compartments of the
 145 biogeochemical module and their interactions (adapted from figures 1 and 2 in Pete et al.,
 146 2020b).

147 Assessments at the watershed/lagoon interface revealed a lack of quantitative data on water and
 148 nutrient loads to the lagoons from surface catchments and groundwater. This observation led
 149 the RMC Water Agency to set up a monitoring network in 2015 to measure pollutant flows to
 150 lagoons with the aim of better quantifying nutrient and chemical contaminant inputs,
 151 particularly during flooding events (AERMC, 2022). This network made it possible to develop
 152 methods to calculate annual water and nutrient loads to the lagoons – methods adapted to
 153 intermittent watercourses subject to flooding phenomena, a major input in Mediterranean
 154 lagoons (Hydriad, 2022). This reinforcement of the monitoring of nutrient flows allowed the
 155 improvement of the GAMELag model’s description of forcing factors at the watershed/lagoon
 156 interface (Figure 1).

157 The results obtained at the first sites where the tool was applied revealed its limitations
 158 (Fiandrino et al., 2022a) and reoriented subsequent studies on the processes involved in the

159 variation of internal nitrogen and phosphorus loads (Figure 1), in particular: (i) the transfer
160 kinetics of nitrogen and phosphorus between the benthic compartment and the water column as
161 a result of sediment stocks and the seasonal variability in this flux (Ouisse et al, 2013); (ii) the
162 dynamic of macrophytes during restoration (Le Fur et al., 2018; 2019) and their capacity to
163 regulate fluxes of matter (Eyre et al., 2011; Le Fur, 2018) and thus reduce sediment release (the
164 concept of storage sustainability).

165 Lastly, a method that estimates the biogeochemical parameters with the most influence in the
166 model, based on global sensitivity analyses, allows optimal combinations of parameter values
167 to be determined (Saguet et al., 2019). Simulations carried out systematically with these
168 different sets of parameters make it possible to associate the water column and phytoplankton
169 metrics with the uncertainties linked to the conceptualisation of the simulated processes. The
170 resulting knowledge has been integrated into the tool (Pete et al., 2017; 2020a) and its use has
171 been tested to establish its efficacy and limitations.

172 *1.5 The tool and its application in the case study of the Or Lagoon*

173 The GAMELag model was developed to evaluate admissible load in French Mediterranean
174 lagoons, serving both as a tool to integrate knowledge acquired in lagoon ecosystems and to
175 support lagoon management agencies that want to adopt an admissible load approach. This
176 article presents a case study of how the GAMELag tool is being used in the specific example
177 of the Or Lagoon, which is the first site where this collaborative approach between managers
178 and scientists has been implemented.

179 For several decades, the Or Lagoon has been one of the most degraded lagoons on the French
180 Mediterranean coast (Derolez et al., 2021; AERMC, 2021). Numerous projects, particularly in
181 terms of wastewater treatment, have been carried out since the early 2000s to reduce nutrient
182 inputs to this lagoon. In 2017, the lack of ecological restoration in this lagoon prompted public
183 authorities (Syndicat Mixte du Bassin de l'Or, SYMBO) to launch a study to better understand

184 the hydrodynamics and ecological functioning of the lagoon and to estimate the admissible
185 nutrient load in this ecosystem.

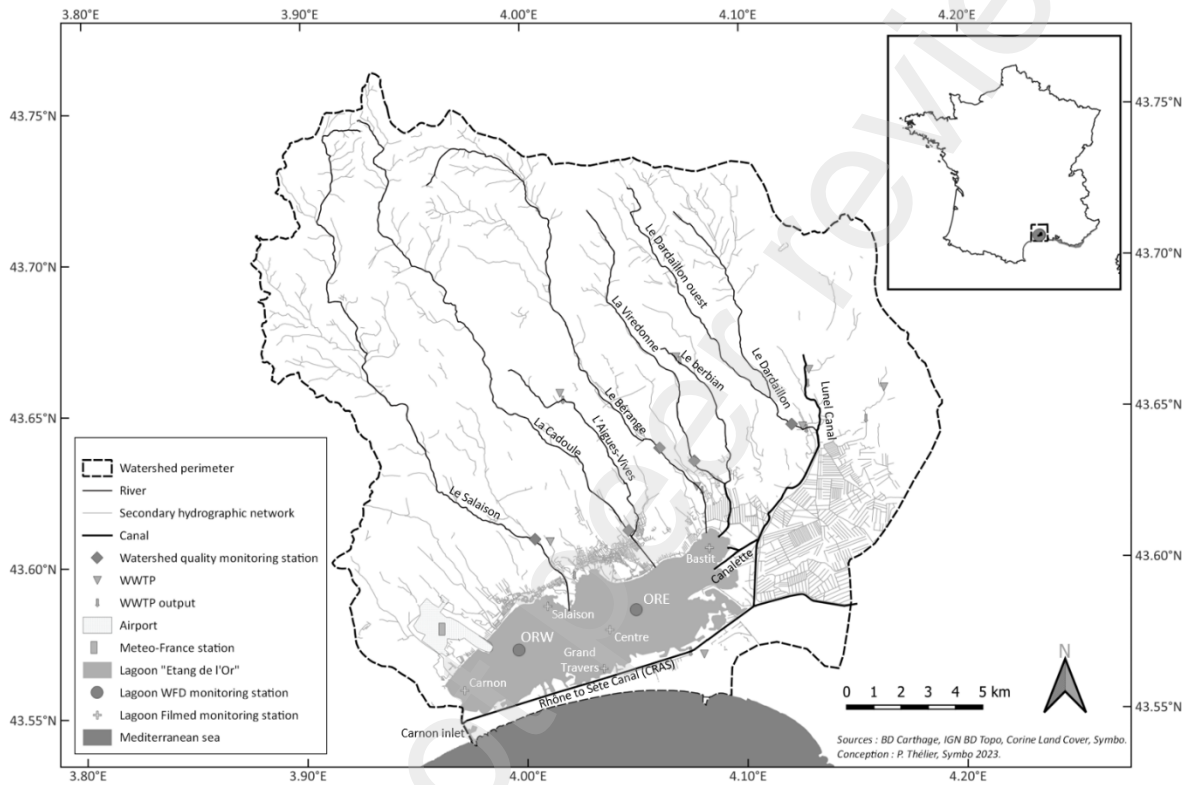
186 **2. Materials and methods**

187 *2.1. Study site: Or Lagoon*

188 The Or Lagoon is located southeast of the city of Montpellier in the south of France near the
189 Mediterranean coastline. It is the third largest lagoon in the region of Occitanie, with a surface
190 area of 3190 ha, an average volume of 50.10^6 m³ and an average depth of 1.3 m (Castaings,
191 2012). The brackish, continental water inputs it receives make it a mesohaline lagoon (average
192 annual salinity $S_{\text{mean}} = 17.3 \pm 6.9$ PSU; SYMBO, pers. comm.). To the south, the Or Lagoon is
193 connected to the Rhône to Sète Canal (CRAS) via the Carnon channel at the southwestern end
194 of the lagoon and three other main channels distributed from west to east along the canal (Figure
195 2). The connection to the sea is indirect via the Carnon inlet, which in turn is connected to the
196 Carnon channel where it intersects the CRAS.

197 To the north and east, the 410 km² catchment area is highly anthropized, with only 6% of natural
198 areas remaining. Most of the land is used for agriculture (around two-thirds of the surface area)
199 and to a lesser extent for urban purposes (~20%). The catchment area is experiencing strong
200 demographic growth (+8% between 2011 and 2020, SYMBO and Acteon, 2021) due to the
201 proximity of the cities of Montpellier and Nîmes and the high level of tourist activities (+50%
202 of the permanent population in the summer period). The tributaries of the Or Lagoon subdivide
203 the area into two parts. The northern watershed (N WS) is drained by four main streams: the
204 Salaison, the Cadoule, the Bérange, and the Viredonne (Figure 2). The eastern watershed is
205 drained by the Lunel Canal, which receives the waters of the Dardaillon, and feeds the lagoon
206 via the Canalette (Figure 2) before flowing, further south, into the CRAS, upstream from the
207 Or Lagoon. Parallel to the lagoon, the CRAS is under the dual influence of marine waters via
208 the Carnon channel to the west and continental waters via the Lunel Canal to the east and the

209 upstream part of the CRAS itself (which is outside the Or Lagoon watershed). The waters of
 210 the CRAS resulting from this mixture are brackish, and their ecological quality is strongly
 211 influenced by the degraded quality of the numerous tributaries that feed it more or less directly,
 212 in particular the Rhône River and the Lunel Canal.



213
 214 Figure 2: Main streams and measuring points in the catchment area and in the Or lagoon.

215 2.2. Application of the GAMELag model to the Or Lagoon

216 We applied the MARS-3D hydrodynamic model to the Or Lagoon (SYMBO, 2019) to define
 217 the number of ‘physical units’ to be considered in the model as suggested by Fiandrino et al.
 218 (2017). We found that a single unit was sufficient to represent the lagoon’s hydrodynamics and
 219 exchanges with the CRAS (results not shown). Moreover, with a turnover time of 87 days and
 220 an average residence time of 117 days (results not shown), the mixing efficiency of this lagoon
 221 (~ 0.74, for a theoretical maximum value equal to 1) is among the highest in Mediterranean

222 lagoons (Umgiesser et al., 2014), confirming that it can be considered a hydrodynamically
223 homogeneous environment.

224 An analysis of monthly salinity measured by SYMBO between 2002 and 2018 at five sites in
225 the Or Lagoon (grey crosses in Figure 2) made it possible to quantify the impact of freshwater
226 inputs via the streams and the Canalette on the lagoon's salinity. Significant differences in
227 salinity were observed between the Bastit site, located at the eastern end of the lagoon, and the
228 other four sites. The largest gradient of salinity (7.7 ± 4.0) was observed between Bastit (S_{mean}
229 $= 12.6 \pm 6.9$) and Carnon, which is located in the extreme west and is influenced by marine
230 water ($S_{\text{mean}} = 20.1 \pm 6.6$). The differences in salinity between the other pairs of sites did not
231 show any marked, stable gradients within the lagoon. Thus, given that the highest desalination
232 is restricted to the zone at the extreme east of the lagoon, we postulated that the Or Lagoon is a
233 single physical unit.

234 This unit receives fresh and brackish water and nitrogen and phosphorus inflows from the N
235 WS and the Canalette (outlet from the eastern watershed into the Or Lagoon) and exchanges
236 water and matter with the CRAS which, in the absence of a direct connection between the
237 lagoon and the sea, represents the 'external marine environment' in the GAMELag tool.

238 *2.3. Forcing dataset for the model*

239 *2.3.1 Atmosphere*

240 The daily time series of air temperature (in °C), relative humidity (in %), wind speed (in $\text{m}\cdot\text{s}^{-1}$)
241 and solar radiation (in $10^6 \text{J}\cdot\text{m}^{-2}\cdot\text{d}^{-1}$) necessary to calculate evaporation and the daily
242 precipitation time series (in $\text{mm}\cdot\text{d}^{-1}$) were acquired from the nearby Montpellier-Fréjorgues
243 meteorological station (Météo-France 43,58°N; 3,96°E; Figure 2) for the period 2013–2018.

244 *2.3.2. Watershed*

245 In the N WS, the Salaison is the only stream in the catchment area equipped with a gauging
246 station for high-frequency flow monitoring (since 1986) (David et al., 2019). The flows of the

247 other streams in this catchment area (Figure 2) were estimated from the daily flow series of the
248 Salaison according to the percentages calculated by Colin et al. (2017): Cadoule (37%),
249 Viredonne (20%), Bérange (18%) and Jasse (4.8%). Nitrogen and phosphorus concentrations
250 in these streams are measured every 15 days (Naiades portal, Watershed quality monitoring
251 stations in Figure 2). Emissions from wastewater treatment plants (WWTPs), which are
252 discharged either directly into the lagoon or into the watercourses downstream of the
253 monitoring points (WWTP in Figure 2), were also taken into account: daily flow data and
254 nitrogen and phosphorus concentrations measured at two-week intervals were provided by the
255 facility managers. In the eastern watershed, the flows and salinity of the Canalette were
256 measured at high frequency (every 10 min) and bimonthly measurements of nitrogen and
257 phosphorus concentrations were acquired over the period from 1 March 2017 to 31 March 2018
258 (SYMBO, 2019).

259 2.3.3. *The Rhône to Sète Canal (CRAS)*

260 The hydrological module of the GAMELag tool, based on the hypothesis that the volume of the
261 lagoon remains constant, simulates the daily net residual volumes (V_R) exchanged with the
262 external environment ($V_R = |V_{In}| - |V_{Out}|$), but does not account for the volume of water that
263 oscillates daily between the lagoon and the external environment (V_{in} and V_{out}). Yet these
264 inflows/outflows, which partly compensate each other diurnally (particularly through tidal
265 action), strongly contribute to the mixing of lagoon and marine waters. To take the impact of
266 this oscillating volume into account, the GAMELag model includes the conceptual mixing
267 volume variable (V_x) defined by Gordon et al. (1996) as a forcing variable. The MARS-3D
268 hydrodynamic model provides the mixing volume time series, defined as the average daily
269 volume exchanged between the lagoon and the CRAS [$V_x = 0.5.(|V_{In}| + |V_{Out}|)$].

270 High-frequency salinity measurements were taken in the CRAS (every 10 min) over the period
271 from 1 March 2017 to 31 March 2018, and the daily averages were used as a forcing condition

272 for the hydrological module (Picard, 2021). Discrete data of concentrations of dissolved
273 inorganic nitrogen, total organic nitrogen, phosphate and total organic phosphorus acquired in
274 the CRAS over the same period were used as forcing conditions for the biogeochemical module
275 (SYMBO, 2019).

276

277 *2.4. Validation of the tool for the Or Lagoon*

278 *2.4.1. Validation of the hydrological module: comparing the salinity measurements to the* 279 *model*

280 The model's ability to reproduce the mixing phenomena between the brackish waters of the
281 lagoon, the marine-influenced waters of the CRAS, and freshwater inputs from the catchment
282 area was evaluated via the temporal changes in salinity simulated in the lagoon on a daily time
283 step between 1 March 2017 and 31 March 2018, the period of the in-situ monitoring. The daily
284 averages of the high-frequency salinity data (acquired every 10 min) from the ORE and ORW
285 sites (Figure 2) were compared to the simulated daily salinity in the physical unit (the lagoon).
286 The performance of the model was analysed using several indices: Root Mean Square Error
287 (RMSE), percent bias (PBias), regression coefficient (R^2) and (dr) index of agreement
288 (Willmott et al., 2012). These statistical indicators were calculated with the hydroGOF package
289 version 0.4-0 in R software.

290 *2.4.2. Parameterisation of the biogeochemical module*

291 The method developed for the GAMELag model to estimate biogeochemical parameters
292 (Saguet et al., 2019) exploits the large number of simulations (several tens of thousands)
293 generated by global model sensitivity analysis methods (Morris, 1991; Saltelli et al., 2000). The
294 state variable values of the biogeochemical module, calculated at a time step of 10 minutes and
295 averaged over the day, were compared with the in-situ data; then the values of the statistical
296 performance indices (identical to those defined for salinity) resulting from these comparisons

297 allowed us to order the simulations and retain the parameterisations (i.e. the combinations of
298 values of the model's 120 parameters), reducing discrepancies between the model's results and
299 the in-situ measurements.

300 The data available for the Or Lagoon are the spot concentrations of dissolved inorganic nitrogen
301 (DIN), total organic nitrogen (TON), total nitrogen (TN), phosphate (PO₄), total organic
302 phosphorus (TOP), total phosphorus (TP) and chlorophyll *a* (chl.*a*) measured annually in the
303 months of June, July and August in 2017 and 2018 at the ORE and ORW sites. These summer
304 data were supplemented by discrete DIN, TON, TN, PO₄, TOP and TP data acquired in the
305 lagoon in January and May 2017 at the same sites (David, 2019). Applying this method for
306 estimating biological parameters in the Or Lagoon resulted in eight different parameterisations,
307 for which 35 parameters differed from their reference values in the literature (results not shown,
308 for more details see Fiandrino et al., 2022a).

309 No in-situ measurements were available for the 'Sediment' and 'Macrophyte' compartments
310 during the validation period. The ability of the model to describe changes in the 'Sediment'
311 compartment was based on total nitrogen and total phosphorus concentration data acquired at
312 15 sites in the Or Lagoon in 2010 (Ifremer, 2011) and 2019. The simulated biomass of
313 opportunistic algae was compared with the biomass value corresponding to the overall
314 eutrophication of the lagoon defined on the basis of the most degraded state simulated for the
315 water column and phytoplankton. The relationship between the ranges of biomass values for
316 opportunistic algae and the global ecological status of a lagoon was provided by the analysis of
317 macrophyte biomass data acquired in 13 lagoons between 2001 and 2006 within the framework
318 of the Regional Lagoon Monitoring Network (Fiandrino et al., 2022b).

319 *2.5. Assessment of admissible load with the GAMELag tool*

320 The method of estimating admissible load is based on exploratory scenario analysis and aims
321 to find the 'balanced ecological functioning of the ecosystem'. This is considered to be the case

322 when (i) the physico-chemical indicators of the water column ([DIN], [DIP], [TN] and [TP])
 323 and the metric associated with phytoplankton biomass meet the ‘good’ status thresholds set by
 324 the WFD (MTES, 2018); (ii) the biomass of opportunistic algae is compatible with the values
 325 observed in lagoons in ‘good’ ecological status (Fiandrino et al., 2022b); (iii) on a yearly scale,
 326 the ecosystem does not store nitrogen and phosphorus in the sediment.

327 Different scenarios of exogenous and possibly endogenous matter inputs via the sediment
 328 compartment were simulated based on forcing conditions characteristic of the current situation.
 329 An exploratory analysis of the results of the simulations revealed the typologies of the functions
 330 characteristic of the ecosystem. Combining the clusters obtained and the constraints of the
 331 ‘balanced ecological functioning of the ecosystem’ defined above resulted in a pressure–state
 332 chart that makes it possible to quantify the ecosystem’s admissible load.

333 2.5.1. Descriptors for ecosystem functioning

334 The descriptors selected to characterise the ecological functioning of the lagoon are listed in
 335 Table 1. Descriptors of the exogenous nitrogen and phosphorus loads that feed the lagoon via
 336 various sources and of the stocks of nitrogen and phosphorus in sediment were also defined to
 337 account for pressures on the ecosystem (Table 2).

338 Table 1: Descriptors of the ecological functioning of the lagoon

<i>Descriptor</i>	<i>Meaning</i>	<i>Unit</i>
$[DIN]_{Lag}$	average summer concentration of dissolved inorganic nitrogen	$mmolN.m^{-3}$
$[DIP]_{Lag}$	average summer concentration of dissolved inorganic phosphorus	$mmolP.m^{-3}$
$[TN]_{Lag}$	average summer concentration of total nitrogen	$mmolN.m^{-3}$
$[TP]_{Lag}$	average summer concentration of total phosphorus	$mmolP.m^{-3}$
$[chl.a]_{Lag}$	average summer concentration of chl.a	$mg\ chl\ a.m^{-3}$
$[Opport]_{Lag}$	average spring biomass of opportunistic species	$gdW.m^{-3}$
$[\Delta TN]_{Sed}$	annual change in nitrogen concentration in the sediment	$mmolN.m^{-2}.y^{-1}$
$[\Delta TP]_{Sed}$	annual change in phosphorus concentration in the sediment	$mmolP.m^{-2}.y^{-1}$
$TN_{Out\ CRAS}$	annual amount of nitrogen exported to CRAS	Tonnes $N.y^{-1}$
$TP_{Out\ CRAS}$	annual amount of phosphorus exported to CRAS	Tonnes $P.y^{-1}$

339

340 Table 2: Descriptors of pressures on the ecosystem

<i>Descriptor</i>	<i>Meaning</i>	<i>Unit</i>
N Load	total annual amount of nitrogen imported into the lagoon via the catchment area and the CRAS	Tonnes N.y ⁻¹
P Load	total annual amount of phosphorus imported into the lagoon via the catchment area and the CRAS	Tonnes P.y ⁻¹
[TN _{Sed}]	initial concentration of nitrogen levels in the sediment	mmol N.m ⁻²
[TP _{Sed}]	initial concentration of phosphorus levels in the sediment	mmol P.m ⁻²

341

342 *2.5.2. Simulation of scenarios (sediment supply/stock) to find optimal functioning*

343 The forcing data defined over a four-year period from 2015 to 2018 and the sediment stock
 344 assessed in 2010 (TN_{Sed} = 12 000 mmol.m⁻² and TP_{Sed} = 724.6 mmol.m⁻², Ouisse et al., 2013)
 345 were used to define the ‘Current’ situation (Table 3). From this initial condition, an
 346 experimental design was constructed in order to test different scenarios in terms of reducing
 347 exogenous inputs from the three sources (the Canalette, the N WS, and the CRAS, Figure 2)
 348 and from the sediment compartment. Decreases in nitrogen and phosphorus inputs from
 349 exogenous sources were made (compared to the ‘Current’ situation) through either a
 350 proportional decrease in nitrogen and phosphorus, or a greater decrease in phosphorus,
 351 modifying the N/P ratio of inputs. The ‘Zero inputs’ scenario (scenario 38: Table 3)
 352 corresponded to an ‘extreme’ situation in which the exogenous inputs from the catchment area
 353 and the CRAS were considered to be nil. Between these two contrasting situations, 37
 354 intermediate scenarios were simulated (scenarios 1 to 37: Table 3). A further 13 scenarios were
 355 simulated by reducing sediment stock in conjunction with reductions in exogenous flows
 356 (scenarios 39 to 51: Table 3). The most restrictive situation for the sediment compartment was
 357 ‘very good’ status (TN_{Sed} = 2721 mmol.m⁻² and TP_{Sed} = 484 mmol.m⁻² as defined by Ouisse et
 358 al., 2020), i.e. Sed_{init} reduction factors of 0.23 for nitrogen and 0.67 for phosphorus. A total of
 359 52 scenarios (including the ‘Current’ situation) were simulated.

360 *2.5.3. Analysis of the scenarios to create a pressure–state chart of the ecosystem*

361 A Principal Component Analysis (PCA) and an Ascending Hierarchical Classification (AHC),
362 carried out with the FactoMineR package in R, allowed an exploration of the values of the
363 descriptors for the 52 simulated scenarios, the four years (2015–2018) and the eight sets of
364 selected parameters (i.e. 1664 independent statistical elements), revealing the typologies of
365 characteristic ecosystem functioning (grouped in clusters).

366 Subsequently, in order to determine a pressure–state chart that links exogenous and endogenous
367 nutrient inputs to the ecological functioning of the ecosystem, ecological criteria were taken
368 into account and a second sub-categorisation was made by considering within each cluster the
369 elements for which: (i) the values of the physicochemical indicators of the water column [DIN],
370 [DIP], [TN], [TP] and the metric associated with phytoplankton biomass [chl.a] were
371 compatible with ‘good’ status (indicated by ‘A’ after the cluster number) and, in contrast;
372 (ii) the values of indicators [TN], [TP] and [chl.a] were representative of ‘poor’ to ‘bad’ status
373 (indicated by ‘D’ after the cluster number); (iii) the ecosystem did not store nitrogen and
374 phosphorus in the sediment (indicated by ‘B’ after the cluster number) and, in contrast; (iv) the
375 ecosystem stored nitrogen or phosphorus in the sediment compartment (indicated by ‘C’ after
376 the cluster number). This allowed the quantification in the pressure–state chart of the
377 ecosystem’s admissible load, i.e. the exogenous inflows admissible for the functioning of the
378 ecosystem compatible with ‘good’ ecological status.

379

380 Table 3: Scenarios for reducing the concentration of exogenous nitrogen and phosphorus
 381 inputs in initial sediment conditions. The values correspond to the reduction coefficients
 382 applied to concentrations in the 'Current' situation (1.00 corresponds to maintaining the initial
 383 values and 0.00 to reducing these to a concentration of zero).

Scenario	NITROGEN				PHOSPHORUS			
	Canalette	Watershed	CRAS	Sed _{Init}	Canalette	Watershed	CRAS	Sed _{Init}
Current	1.00	1.00	1.00	1.00	1.00	1.00	1.00	1.00
1	1.00	1.00	0.93	1.00	1.00	1.00	0.58	1.00
2	1.00	1.00	0.93	1.00	1.00	1.00	0.30	1.00
3	1.00	1.00	0.47	1.00	1.00	1.00	0.29	1.00
4	1.00	1.00	0.47	1.00	1.00	1.00	0.13	1.00
5	1.00	1.00	0.23	1.00	1.00	1.00	0.15	1.00
6	1.00	1.00	0.23	1.00	1.00	1.00	0.07	1.00
7	1.00	1.00	0.12	1.00	1.00	1.00	0.07	1.00
8	1.00	1.00	0.12	1.00	1.00	1.00	0.03	1.00
9	1.00	1.00	0.06	1.00	1.00	1.00	0.01	1.00
10	0.59	1.00	1.00	1.00	0.27	1.00	1.00	1.00
11	0.59	1.00	1.00	1.00	0.20	1.00	1.00	1.00
12	0.59	1.00	0.93	1.00	0.27	1.00	0.58	1.00
13	0.59	1.00	0.93	1.00	0.20	1.00	0.30	1.00
14	0.59	0.75	0.93	1.00	0.27	0.75	0.58	1.00
15	0.59	0.75	0.93	1.00	0.20	0.55	0.30	1.00
16	0.29	1.00	1.00	1.00	0.14	1.00	1.00	1.00
17	0.29	1.00	1.00	1.00	0.08	1.00	1.00	1.00
18	0.29	1.00	0.47	1.00	0.14	1.00	0.29	1.00
19	0.29	1.00	0.47	1.00	0.08	1.00	0.13	1.00
20	0.29	0.50	0.47	1.00	0.14	0.50	0.29	1.00
21	0.29	0.50	0.47	1.00	0.08	0.35	0.13	1.00
22	0.15	1.00	1.00	1.00	0.07	1.00	1.00	1.00
23	0.15	1.00	1.00	1.00	0.04	1.00	1.00	1.00
24	0.15	1.00	0.23	1.00	0.07	1.00	0.15	1.00
25	0.15	1.00	0.23	1.00	0.04	1.00	0.07	1.00
26	0.15	0.75	0.23	1.00	0.07	0.75	0.15	1.00
27	0.15	0.75	0.23	1.00	0.04	0.55	0.07	1.00
28	0.07	1.00	1.00	1.00	0.03	1.00	1.00	1.00
29	0.07	1.00	1.00	1.00	0.02	1.00	1.00	1.00
30	0.07	1.00	0.12	1.00	0.03	1.00	0.07	1.00
31	0.07	1.00	0.12	1.00	0.02	1.00	0.03	1.00
32	0.07	0.50	0.12	1.00	0.02	0.35	0.03	1.00
33	0.07	0.25	0.12	1.00	0.02	0.17	0.03	1.00
34	0.04	1.00	1.00	1.00	0.01	1.00	1.00	1.00
35	0.04	1.00	0.06	1.00	0.01	1.00	0.01	1.00
36	0.04	0.15	0.06	1.00	0.01	0.05	0.01	1.00
37	0.00	0.00	1.00	1.00	0.00	0.00	1.00	1.00
38	0.00	0.00	0.00	1.00	0.00	0.00	0.00	1.00
39	1.00	1.00	1.00	0.84	1.00	1.00	1.00	0.95
40	0.00	0.00	0.00	0.84	0.00	0.00	0.00	0.95
41	1.00	1.00	1.00	0.50	1.00	1.00	1.00	0.50
42	0.04	0.15	0.06	0.50	0.01	0.05	0.01	0.50
43	0.00	0.00	0.00	0.50	0.00	0.00	0.00	0.50
44	0.59	1.00	1.00	0.23	0.20	1.00	1.00	0.67
45	1.00	1.00	1.00	0.23	1.00	1.00	1.00	0.67
46	1.00	1.00	0.47	0.23	1.00	1.00	0.13	0.67
47	0.29	1.00	1.00	0.23	0.08	1.00	1.00	0.67
48	0.29	1.00	0.47	0.23	0.08	1.00	0.13	0.67
49	0.29	0.50	0.47	0.23	0.08	0.35	0.13	0.67
50	0.00	1.00	0.00	0.23	0.00	1.00	0.00	0.67
51	0.00	0.00	0.00	0.23	0.00	0.00	0.00	0.67

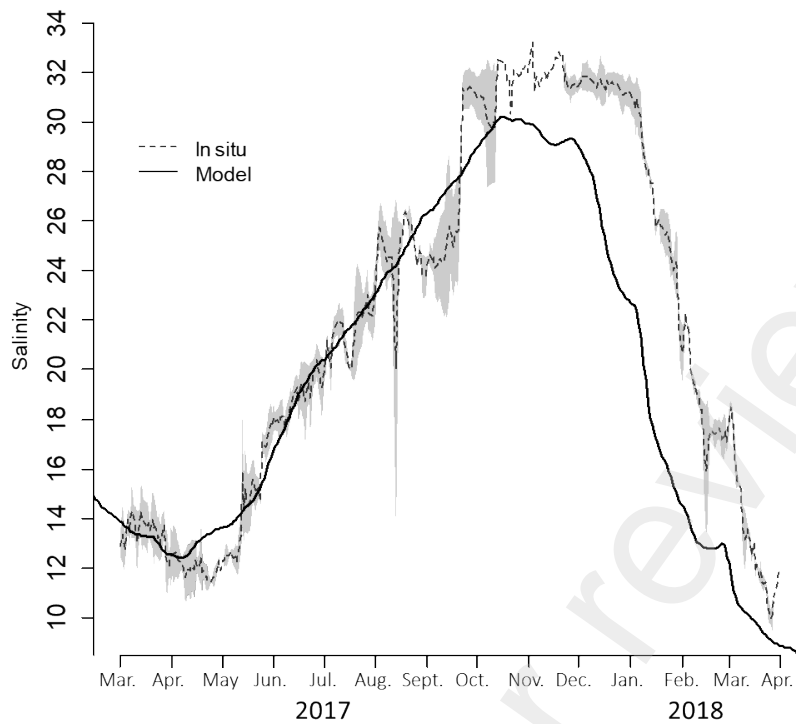
384

385 **3. Results**

386 *3.1. Model's ability to reproduce mixing phenomena*

387 A comparison between measured and simulated salinity over the period from 1 March 2017 to
388 31 March 2018 showed that the model correctly reproduced the general trend (Figure 3). The
389 increase in salinity between early April and mid-October 2017 was replicated well by the model
390 ($r^2 = 0.96$; $d = 0.99$, bias = -1.2%). The very low inflow of fresh water from the catchment area
391 ($26.4 \cdot 10^6 \text{ m}^3$) and very low direct precipitation falling on the lagoon ($7.5 \cdot 10^6 \text{ m}^3$), as well as the
392 significant evaporation ($-26.5 \cdot 10^6 \text{ m}^3$) over this 7-month period, explain the particularly high
393 salinity values reached in autumn 2017 (>30).

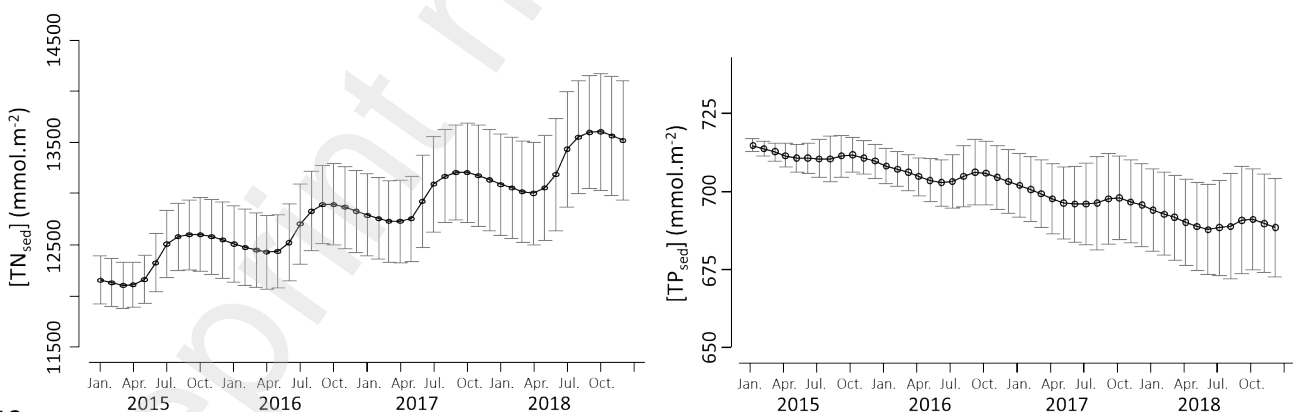
394 The significant drop in salinity ($\Delta S = -20$ between the beginning of December 2017 and the end
395 of March 2018) was also well reproduced by the model, although in advance ($r^2 = 0.89$; $d =$
396 0.84 , bias = -24.4%). The rainfall that occurred between the beginning of December 2017 and
397 the beginning of January 2018 resulted, in the model forcing, in significant freshwater inputs
398 ($26.4 \cdot 10^6 \text{ m}^3$ from the catchment area and $2.4 \cdot 10^6 \text{ m}^3$ from direct rainfall on the lagoon), which
399 led to a decrease in the simulated salinity. This first rainfall after a long dry period had little
400 impact on measured salinity in the lagoon. The drop in salinity was only observed from mid-
401 January 2018 after heavy rainfall followed by a very wet end of winter. Over the period from
402 mid-January to the end of March 2018, freshwater inflows from the catchment area were
403 estimated at $48.8 \cdot 10^6 \text{ m}^3$ and from direct rainfall on the lagoon at $12.0 \cdot 10^6 \text{ m}^3$.



404
 405 Figure 3: Change in salinity over the period from 1 March 2017 to 31 March 2018: model
 406 simulation shown by the black solid line and high-frequency in-situ measurements taken at the
 407 ORW and ORE sites shown in grey (grey dashes = mean value).

408 *3.2. Model's ability to reproduce changes in the sediment stock of nitrogen and phosphorus*

409 The model simulated an increase in nitrogen stock in the first 5 cm of sediment (Figure 4, left)
 410 of +334 mmol N.m⁻².y⁻¹ and a slow decrease in the sediment stock of phosphorus (Figure 4,
 411 right) of -6.8 mmol P.m⁻².y⁻¹.

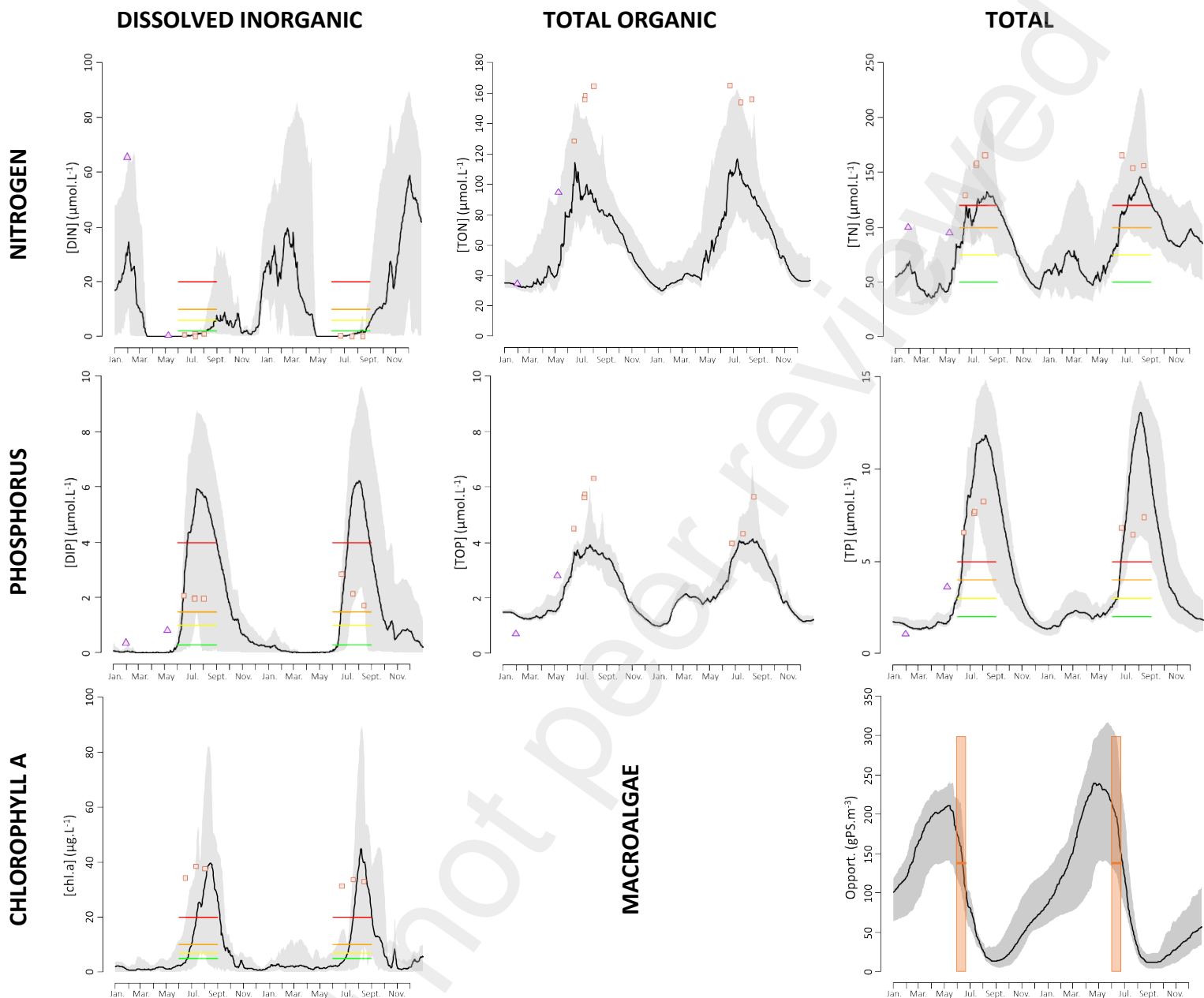


412
 413 Figure 4: Simulated monthly change in nitrogen and phosphorus sediment stocks between
 414 2015 and 2018. The dots represent the means and the error bars the standard deviations of the
 415 values obtained from the eight parameterisations used in the model.

416 The simulated increase in nitrogen stock was not in line with observations, which showed a
417 significant decrease between 2010 and 2019 [$\Delta\text{TN}_{\text{Sed}}$]₂₀₁₉₋₂₀₁₀ = -1976.2 ± 2112.1 mmol N.m⁻²
418 (p-value < 0.1). However, the model correctly accounted for the change in the sediment stock
419 of phosphorus. Over the period 2010 and 2019, the simulated difference in phosphorus stock (-
420 61 mmolP.m⁻² extrapolating the results obtained during 2015–2018) was in line with
421 observations ([$\Delta\text{TP}_{\text{Sed}}$]₍₂₀₁₉₋₂₀₁₀₎ = -41.2 ± 131.3 mmol P.m⁻²).

422 3.3. Model's ability to reproduce ecological functioning of the lagoon

423 The model's inability to simulate the change in the sediment stock of nitrogen over the medium
424 to long term does not call into question its ability to account for changes in the water column,
425 phytoplankton and macrophyte parameters. Indeed, the model satisfactorily reproduced the
426 ecological functioning of the lagoon in the summer period, showing excessive primary
427 production limited by the availability of dissolved inorganic forms of nitrogen and an excess of
428 phosphate in the water column (Figure 5). The summer phosphate concentration was, on
429 average, overestimated by a factor of two over the eight simulations (bias = 110%), and the
430 summer organic phosphorus concentration was underestimated (bias = -26.4%), with a
431 consequent overestimation of total phosphorus concentration (bias = 32.9%). The summer
432 concentration of inorganic nitrogen was on average overestimated by the model over the eight
433 simulations (bias = +87.7%), particularly in August, but this overestimation must be put into
434 perspective due to the very low values below the 'very good'/'good' threshold (green line on
435 Figure 5). Dissolved organic nitrogen concentration was underestimated (bias = -34.8%) with
436 a direct impact on total nitrogen concentration (bias = -20%). However, taking into account the
437 uncertainties of the model, it can be considered that it gave a reasonable representation of the
438 measured values of these four parameters (Figure 5).



439 Figure 5: Temporal change in the parameters DIN, TON, TN, DIP, TOP, TP and chl.a
 440 simulated between 1 January 2016 and 31 December 2018. The solid line corresponds to the
 441 average of the results obtained with the eight parameter sets and the shaded area is defined by
 442 the minimum and maximum values. WFD monitoring data (squares), discrete data (triangles),
 443 and the lower thresholds of the WFD status classes are also represented ('Good': green line;
 444 'Average/Fair': yellow line; 'Poor': orange line; 'Bad': red line). On the macroalgae graph,
 445 the orange bars show the mean values and standard deviations of the biomass characteristic of
 446 a poor state.

447 The model simulated a phytoplankton bloom between the months of June and October with a
 448 chlorophyll *a* peak in August, the average intensity of which over the eight simulations was
 449 comparable to observations (35 to 45 $\mu\text{g.L}^{-1}$). The underestimation of the simulated chlorophyll
 450 concentration in June suggests, however, that the estimated start of the bloom was somewhat

451 late. The simulated biomass of opportunistic algae was minimal in early autumn, increased to
452 its maximum value between March and May ($\sim 200 \text{ gPS.m}^{-3}$ in 2017 and 250 gPS.m^{-3} in 2018)
453 and then decreased rapidly in June. In 2017, the simulated biomass was in line with the biomass
454 value corresponding to a lagoon in 'poor' to 'bad' status (orange bars defined based on
455 Fiandrino et al., 2022b). In 2018, the simulated algal bloom was larger, and the biomass was in
456 the high range of the descriptor.

457 *3.4. Matter and water balance*

458 The water balance and matter balance for 2015 to 2018 (Table 4) showed high interannual
459 variability of inputs linked to variation in precipitation, which influences the flow of streams in
460 the natural catchment area (northern watershed, Table 4) and, to a lesser extent, the flow of the
461 Canalette. Freshwater inflow from the N WS was almost three times higher in a wet year (2018)
462 than in a dry year (2017). For the Canalette, which is the main source of water in the catchment
463 area, the factor between wet and dry years was 1.9: it accounted for 62% of inflow in wet years
464 and 79% in dry years.

465 Nitrogen and phosphorus inputs from the catchment area (Watershed, Table 4) also showed
466 high interannual variability (factor of 2.6 for nitrogen and 2.4 for phosphorus between dry and
467 wet years). The N:P mass ratio of inputs from the N WS varied around 46.6 ± 15 , with the
468 highest values in dry years and the lowest in wet years. The N:P mass ratio from the Canalette
469 was much more stable at around 10 ± 0.8 . This stable, marked imbalance in phosphorus from
470 the Canalette made it the lagoon's main source of phosphorus, with a contribution to the input
471 from the catchment area that varied between 73% in wet years and 88% in dry years. However,
472 while the Canalette was also the main source of nitrogen in the watershed in a dry year (79%),
473 the N WS became the main source in a wet year, with 55% of the nitrogen input.

474 Nitrogen and phosphorus inputs from the CRAS (CRAS In, Table 4) showed low interannual
 475 variability (factor of 1.3 for nitrogen and 1.2 for phosphorus between dry and wet years). The
 476 contribution of CRAS to total annual nitrogen input (336 Tonnes N.y⁻¹) was predominant in dry
 477 years (66%) and represented more than one-third of total annual inputs in wet years (457
 478 Tonnes N.y⁻¹). The CRAS's contribution to total annual phosphorus inputs (26 Tonnes P.y⁻¹)
 479 was even more marked and represented nearly 71% in a dry year and nearly 47% of the 33.5
 480 Tonnes P.y⁻¹ that the lagoon received in a wet year.

481 The net balance of matter between the lagoon and the CRAS was in equilibrium in dry years
 482 (Inputs/Outputs: I/O_N^{CRAS} = -6 ± 39 Tonnes N.y⁻¹; I/O_P^{CRAS} = -7 ± 6 Tonnes P.y⁻¹) and strongly
 483 tipped to matter export in wet years (I/O_N^{CRAS} = -161 ± 47 Tonnes N.y⁻¹; I/O_P^{CRAS} = -16 ± 6
 484 Tonnes P.y⁻¹). The annual matter balance on the scale of the lagoon was positive: i.e. nitrogen
 485 and, to a lesser extent, phosphorus tended to accumulate in the lagoon whatever the hydrological
 486 conditions (I/O_N^{LAG} = +136 ± 47 Tonnes N.y⁻¹; I/O_P^{LAG} = +4 ± 7 Tonnes P.y⁻¹).

487 Table 4: Annual balance of water, nitrogen and phosphorus inputs to the Or Lagoon from the
 488 atmosphere, the watershed (N WS = northern watershed) and the Rhône to Sète Canal
 489 (CRAS) from 2015–2018. The years in brackets are associated with the minimum and
 490 maximum values for each parameter. For the import/export of matter by CRAS, the values
 491 correspond to the average and the standard deviation of the eight sets of parameters.

WATER (10 ⁶ m ³ .y ⁻¹)							
ATMOSPHERE		WATERSHED				CRAS	
Rainfall	Evaporation	Watershed	Canalette	N WS	WWTP	In	Out
10.3 - 30.9 (2017) - (2018)	25.8 - 28.1 (2016) - (2017)	56.2 - 122.0 (2017) - (2018)	40.0 - 75.4 (2017) - (2018)	15.3 - 46.6 (2017) - (2018)	0.07 - 0.08 (2016) - (2017)	162.2 - 203.1 (2018) - (2017)	243.1 - 289.7 (2017) - (2018)

NITROGEN (Tons.y ⁻¹)							
ATMOSPHERE		WATERSHED				CRAS	
Rainfall	Evaporation	Watershed	Canalette	N WS	WWTP	In	Out
3.1 - 9.5 (2017) - (2018)	- -	114.6 - 291.1 (2017) - (2018)	60.1 - 171.0 (2017) - (2016)	46.0 - 160.5 (2016) - (2018)	0.3 - 0.5 (2017) - (2015)	165.5 - 221.1 (2018) - (2017)	227.5 ± 39.8 / 326.5 ± 47.3 (2017) / (2018)

PHOSPHORUS (Tons.y ⁻¹)							
ATMOSPHERE		WATERSHED				CRAS	
Rainfall	Evaporation	Watershed	Canalette	N WS	WWTP	In	Out
0.2 - 0.7 (2017) - (2018)	- -	7.5 - 17.8 (2017) - (2016)	6.6 - 16.4 (2017) - (2016)	0.8 - 4.3 (2017) - (2018)	0.05 - 0.09 (2018) - (2015)	15.7 - 18.4 (2018) - (2017)	25.8 ± 5.7 / 31.4 ± 5.6 (2017) / (2018)

493 3.5. Matter fluxes between the compartments of the ecosystem

494 The outcome of exogenous inputs in the ecosystem was analysed in terms of storage and matter
495 fluxes exchanged between the different compartments of the ecosystem (Figure 6). The nitrogen
496 and phosphorus stocks in the hydrobiological compartments (coloured circles) corresponded to
497 annual averages. In the sediment, the values corresponded to the difference in nitrogen and
498 phosphorus stocks between the end and the beginning of each year. The nitrogen and
499 phosphorus fluxes between the compartments were cumulated over a year. The variation in
500 stocks and annual fluxes was averaged over the four simulated years and the eight
501 parameterisations.

502 *3.5.1 'Current' situation*

503 Internal sources (biological compartments and sediment) accounted for 73% of dissolved
504 inorganic nitrogen inputs to the water column, with little interannual variability but seasonal
505 variation (from 43% in winter to 96% in summer). From October to June, fluxes from sediment
506 release were the main internal source of DIN (66%) and in summer, remineralisation of organic
507 matter in the water column became predominant (48% from internal sources). Exogenous inputs
508 accounted for an average of 23% of DIN inputs, more than two-thirds of which came from the
509 catchment area (N WS and Canalette).

510 Internal sources also accounted for the majority of dissolved inorganic phosphorus. These
511 endogenous sources represented more than 80% of inputs with seasonal variation (from 64% in
512 winter to 91% in summer). Between May and July, the mortality of opportunistic algae was the
513 main internal source of DIP (47%), and then in August–September the mineralisation of organic
514 matter in the water column became predominant. For the rest of the year, sediment release was
515 the main internal source of DIP (65%). Inputs from the catchment area and the CRAS
516 represented at most 10% of the inputs (in wet years from the catchment area, and in dry years
517 from the CRAS).

518 Opportunistic algae was primarily responsible for the assimilation of inorganic nitrogen: 57%
519 was assimilated by algae compared to 38% for phytoplankton. The distribution was more
520 balanced for phosphate, macrophytes and phytoplankton, which each assimilated around 48%.
521 This assimilation of matter by macroalgae and phytoplankton was clearly staggered in time,
522 with storage of matter (nitrogen and phosphorus) mainly in the 'Phytoplankton' compartment
523 from July to September, and then storage in the 'Macroalgae' compartment from October to
524 November, reaching a maximum in April before a decrease in June. Thus, the primary role of
525 macroalgae and phytoplankton in the assimilation of inorganic nitrogen and phosphorus was
526 reversed between June and July.

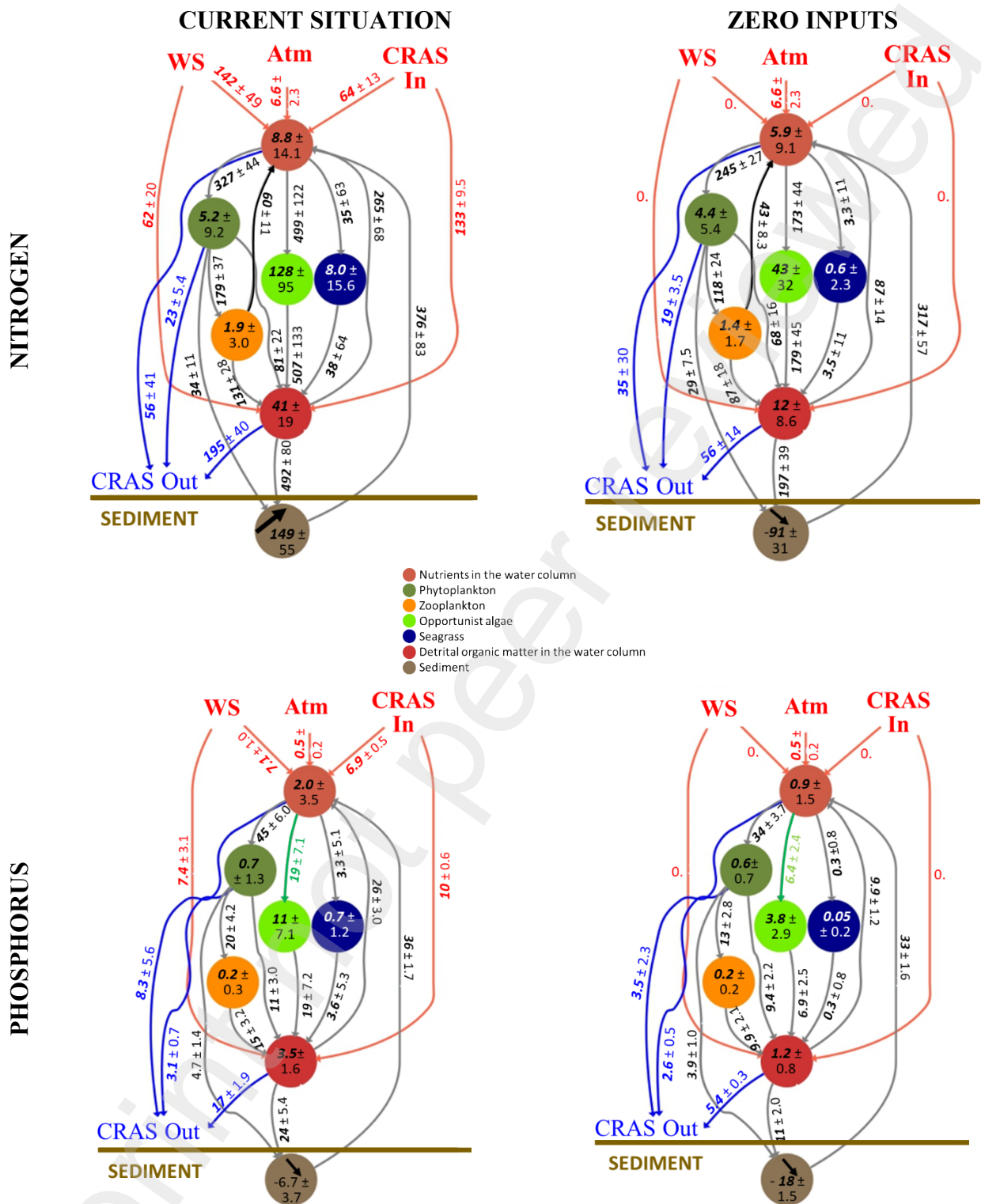
527 Exports of dissolved inorganic forms to the CRAS accounted for only 6% of DIN losses to the
528 water column, compared to almost 11% for DIP. For DIN, exports were highest in winter
529 (December to February), while DIP exports were highest in summer (June to September). This
530 difference indirectly reflects the role of DIN as a limiting factor in primary production,
531 particularly in the summer period.

532 Concerning detrital organic forms, internal sources accounted for nearly 80% of nitrogen inputs,
533 53% of which were derived from the degradation of opportunistic algae. The degradation of
534 zooplankton and phytoplankton represented less than 14% and 9% of internal sources
535 respectively. Exogenous inputs of nitrogen were mostly associated with CRAS (14%).

536 Internal sources accounted for almost 74% of detrital organic phosphorus inputs, of which 29%,
537 22% and 17% came from the degradation of opportunistic algae, zooplankton and
538 phytoplankton respectively. As for nitrogen, exogenous inputs were primarily associated with
539 CRAS (15%).

540 Exports of detrital organic forms to CRAS accounted for almost 29% of nitrogen losses and
541 40% of phosphorus losses.

542



543 Figure 6: Representation of simulated stocks and fluxes of nitrogen (top) and phosphorus
 544 (bottom) for the ‘Current’ situation (left) and for a ‘Zero inputs’ from the watershed scenario
 545 (right). The arrows represent the cumulative annual fluxes (expressed in Tonnes.y⁻¹) between
 546 the different compartments. The green arrows correspond to a net balance of bilateral
 547 phosphate exchange between the ‘DIP’ and ‘Macroalgae’ compartments. The circles represent
 548 the average annual stocks (expressed in tonnes) in the compartments, except for the
 549 ‘Macrophyte’ compartment, in which the values represent the spring stocks (in tonnes), and
 550 the sediment compartment, in which the values correspond to the difference between the stock
 551 at the beginning and end of the year (in tonnes).

552 The degradation of organic matter accounted for almost 94% and 83% of the sources of
553 sediment nitrogen and phosphorus respectively. This flux of nitrogen towards the sediment
554 showed strong seasonal variability, with more than 48% of the annual flux generated in the
555 summer period compared to less than 5% in winter. The magnitude of seasonal variation in the
556 remineralisation fluxes of organic matter in the sediment (nitrogen losses in the sediment
557 compartment) was lower, fluctuating between 35% in summer and 17% in winter. Thus,
558 between October and March, there was a greater outflow of nitrogen leaving sediment than
559 inflow, explaining the decrease in simulated stocks over this period; however, the marked
560 differences in intensity in which inflow was greater from April to September were responsible
561 for the overall tendency for nitrogen to be stored in the sediment compartment (Figure 6, left).
562 Phosphorus fluxes exchanged between water and sediment showed the same seasonal changes
563 as nitrogen fluxes, but the intensity of summer fluxes into and out of the sediment were of the
564 same order of magnitude. Thus, the very low phosphorus storage simulated in the summer
565 period did not compensate for the differences due to phosphorus release simulated in the periods
566 from October to May (Figure 6, right).

567 3.5.2 'Zero inputs' scenario

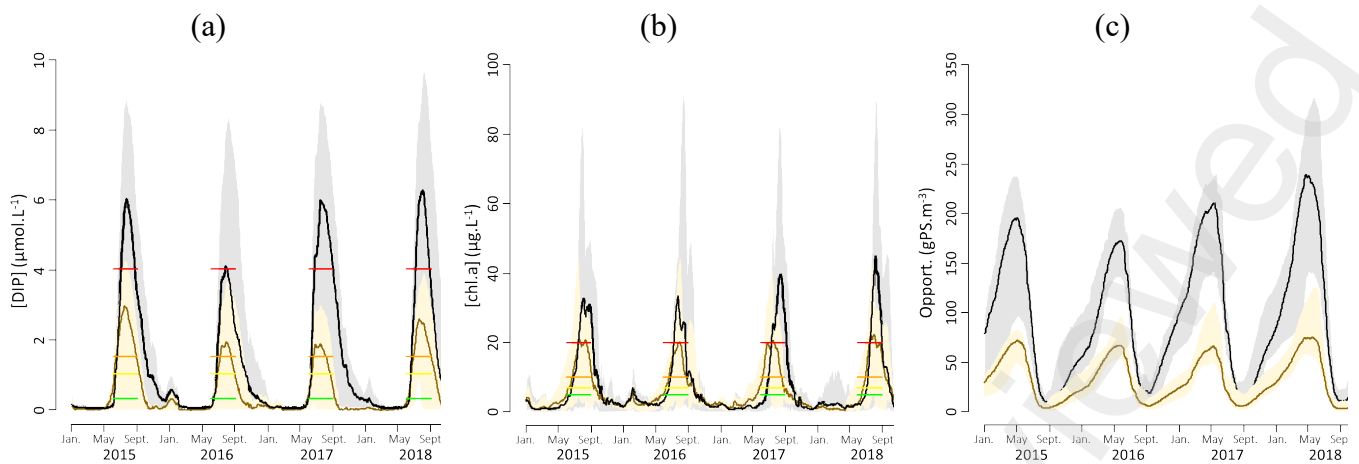
568 In the scenario where inputs from the catchment area and CRAS were set to zero (scenario 38,
569 Table 3), the functioning of the system was strongly modified. Compared to the 'Current'
570 situation, the endogenous inputs of DIN and DIP decreased by a factor of 0.64 and 0.7
571 respectively, due to a marked reduction in the remineralisation processes of organic matter
572 directly in the water column (factor of 0.34 for DIN and 0.39 for DIP). Summer stocks of DIP
573 in the water column were greatly reduced (by a factor of 0.42), but remained characteristic of a
574 'poor' biological status with regard to the WFD indicators (Figure 7). As nitrogen remained the
575 limiting factor in primary production, the summer stock of DIN in the water column was not
576 significantly different between the two scenarios.

577 The assimilation of nutrients by opportunistic algae was also strongly impacted by removing
578 exogenous inputs, reducing the quantities of nitrogen and phosphorus stored by these species
579 in spring by a factor of 0.35. The maximum biomass of opportunistic algae was 75 g PS.m^{-3}
580 compared to more than 200 g PS.m^{-3} in the 'Current' situation (Figure 7).

581 Nutrient uptake by phytoplankton was less impacted in the 'Zero inputs' scenario, reducing this
582 by a factor of 0.75 compared to the 'Current' situation. Summer primary production remained
583 excessive, with chlorophyll biomass still characteristic of 'bad' biological status (Figure 7).

584 This reduction in stocks of living matter resulted in a marked decrease in endogenous nitrogen
585 and phosphorus fluxes to the organic compartment (by a factor of 0.45 for organic nitrogen and
586 0.54 for organic phosphorus), which was reflected in sedimentation fluxes (reduction by a factor
587 of 0.43 for nitrogen and 0.54 for phosphorus). While the diffusion of nutrients from sediment
588 to the water column was the process least impacted by the 'Zero inputs' scenario (reduction by
589 a factor of 0.85 for DIN and 0.93 for DIP), the net balance of water–sediment exchanges was
590 still strongly modified. The depletion of phosphorus, also simulated in the 'Current' situation,
591 increased by a factor of 3.5 in the 'Zero inputs' scenario, and a major change in the functioning
592 of the ecosystem was simulated with regard to the level of nitrogen, with a reversal of the trend
593 and a depletion of nitrogen in sediment (Figure 6).

594



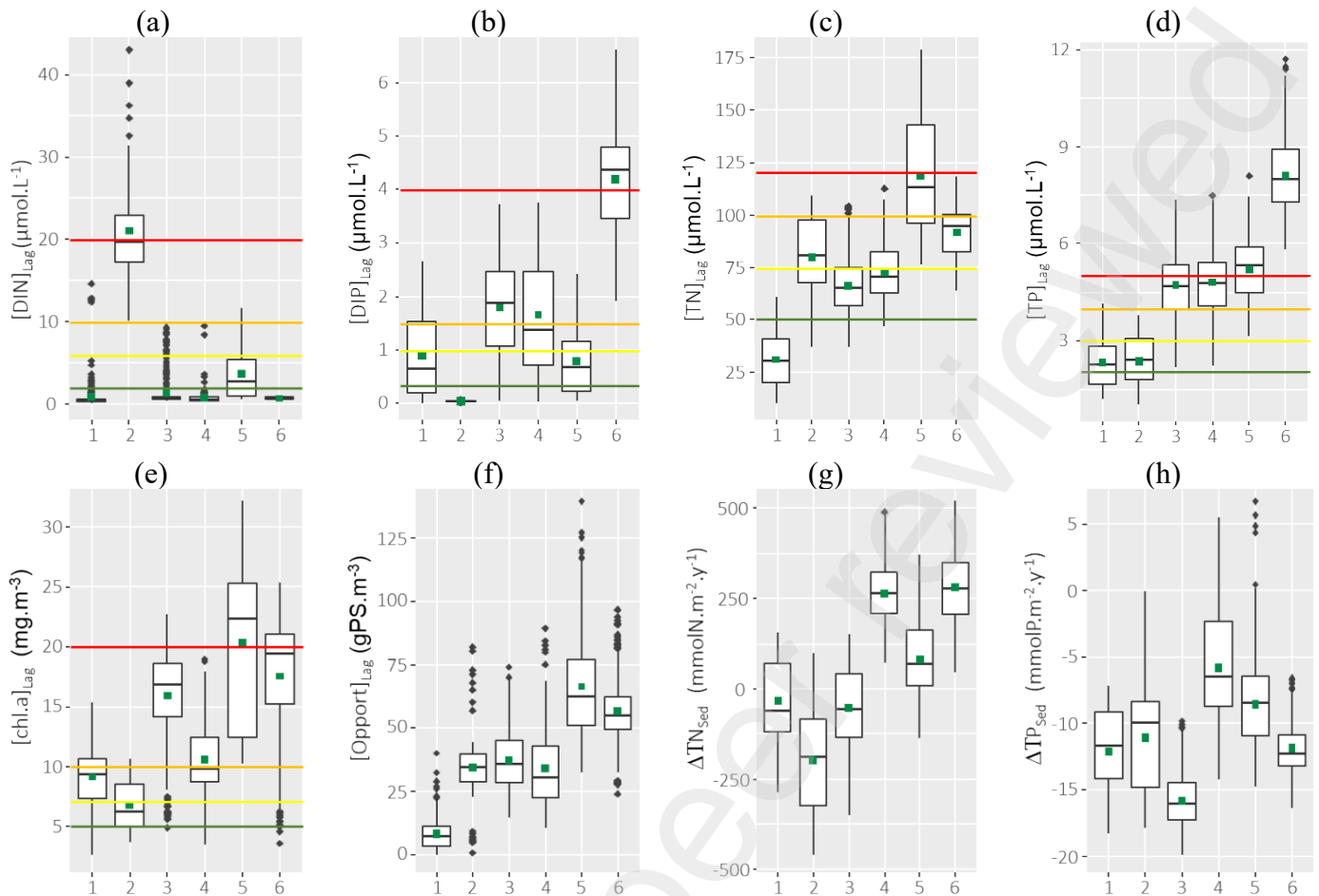
595 Figure 7: Temporal variations in DIP (a), chl.a (b) and opportunistic algal biomass (c) for the
 596 two scenarios ‘Current’ situation (black line and grey shading) and ‘Zero inputs’ (brown line
 597 and yellow shading). The lower thresholds of the WFD status classes (‘Good’: green line;
 598 ‘Average/Fair’: yellow line; ‘Poor’: orange line; ‘Bad’: red line) are also shown.

599 3.6. Typologies of ecosystem functioning: clustering results

600 The exploratory analysis of 52 scenarios (Table 3) and 1664 independent statistical elements
 601 was grouped into six clusters associated with types of ecological functioning (Figure 8). Four
 602 clusters (1, 3, 4, 6) were characteristic of ecosystem functioning in which nitrogen is the limiting
 603 parameter for biological production, with very low summer concentration of dissolved
 604 inorganic nitrogen (Figure 8a). Cluster 1 grouped elements (n=205) for which chlorophyll *a*
 605 concentrations (Figure 8e), biomass of opportunistic algae (Figure 8f) and summer stocks of
 606 total nitrogen and total phosphorus (Figure 8c, d) in the water column were among the lowest.
 607 Annual sediment stocks of nitrogen [ΔTN_{sed}] and phosphorus [ΔTP_{sed}] (Figure 8g, h) decreased.
 608 Cluster 6 grouped the elements (n=410) in which the concentrations of dissolved inorganic
 609 phosphorus and total phosphorus in the water column (Figure 8b, d) were highest. This type of
 610 ecosystem was very productive, with concentrations of chlorophyll *a* and opportunistic algae
 611 biomass also among the highest (Figure 8e, f). The matter produced tended to be stored in the
 612 sediment, with large annual increases in sediment nitrogen stocks (Figure 8g).
 613 Clusters 3 (n=531) and 4 (n=188) grouped elements that lay in between clusters 1 and 6 with
 614 respect to dissolved inorganic phosphorus and total phosphorus concentrations (Figure 8b, d).

615 The production of opportunistic algae remained moderate, with average biomass of less than
616 50 g PS.m⁻³ (Figure 8f). Chlorophyll biomass was high for cluster 3, with values that were on
617 average in the middle of the poor category (Figure 8e). In cluster 4, predation by zooplankton
618 limited phytoplankton production, but the organic matter produced was largely stored in the
619 sediment (Figure 8g).

620 Cluster 2 grouped elements (n=59) in which the summer concentration of dissolved inorganic
621 nitrogen was highest (Figure 8a). Primary production was limited by the availability of
622 phosphate in the water column (Figure 8b). Chlorophyll *a* concentration was among the lowest,
623 and biomass of opportunistic algae was moderate (Figure 8e, f). Annual stocks of nitrogen and
624 phosphorus in the sediment decreased (Figure 8g, h).



625 Figure 8: Distributions for the 1664 statistical elements of the values of 8 ecosystem
 626 descriptors (Table 1) within the 6 clusters identified by the AHC following the PCA: (a) DIN;
 627 (b) DIP; (c) TN; (d) TP; (e) chl.a; (f) opportunistic species; (g) annual change in sediment
 628 nitrogen stock; (h) annual change in sediment phosphorus stock. The horizontal lines
 629 represent the WFD thresholds when they exist (green: ‘Very Good’/‘Good’ threshold; yellow:
 630 ‘Good’/‘Fair’ threshold; orange: ‘Fair’/‘Poor’ threshold; red: ‘Poor’/‘Bad’ threshold).

631 Cluster 5 grouped elements ($n=271$) in which the chlorophyll *a* concentration (Figure 8e),
 632 biomass of opportunistic algae (Figure 8f) and the summer stock of total nitrogen in the water
 633 column were highest (Figure 8c). Annual nitrogen stock in the sediment tended to increase
 634 (Figure 8g).

635 3.7. Creation of a pressure–state chart to support lagoon management

636 The combination of the six clusters with the WFD thresholds of the water column and
 637 phytoplankton parameters and the change in the sediment stock resulted in the distribution of
 638 the 1664 elements in 16 sub-clusters (Table 5). The sub-clusters represented the ranges of
 639 variation in exogenous (northern and eastern watersheds and CRAS) and endogenous

640 (sediment) pressures in relation to the response of hydrobiological parameters in the lagoon,
 641 providing a pressure–state chart that links the pressures experienced by the lagoon with its
 642 ecological state. For the sake of readability, Figure 9 shows the nine sub-clusters that were most
 643 contrasting (in terms of ecosystem functioning) and most representative (in terms of numbers
 644 of elements in the cluster).

645 Table 5: Distribution of the 1664 elements in the 16 sub-clusters resulting from the
 646 combination of the 6 clusters (in rows) and the 4 constraints (in columns) imposed on the
 647 water column/phytoplankton and sediment compartments (see §2.5.3. for the definition of
 648 conditions A,B,C,D). The 9 underlined/bold sub-clusters correspond to the sub-clusters
 649 retained to determine the pressure–state chart (Figure 9).

Cluster	WFD Cond.	Water / Phytoplankton status			
		Good	Intermediate	Bad	
		Sediment			
			No stock	Stock	
	A	B	C	D	
1	<u>23</u>	<u>113</u>	<u>69</u>		
2		55	4		
3		<u>293</u>	<u>138</u>	100	
4	3		<u>159</u>	26	
5		<u>22</u>	23	<u>226</u>	
6			76	<u>334</u>	

650

651 Elements corresponding to the ‘Current’ situation were mainly grouped in sub-clusters 6D (63%
 652 of cases) and 5D (22% of cases). These two sub-clusters were characteristic of ecosystem
 653 functioning in which exogenous inputs (on the order of 316 ± 72 Tonnes $N.y^{-1}$ and
 654 19.5 ± 6.4 Tonnes $P.y^{-1}$) and current sediment stock (poor state for nitrogen and average/fair state
 655 for phosphorus) (Figure 9, ‘Pressures’) supported excessive phytoplankton production and
 656 significant blooms of opportunistic algae (Figure 9, ‘State’). The ecosystem stored nitrogen in
 657 the sediment compartment.

658 Assuming that ‘current’ exogenous inputs are associated with initial sediment stocks
 659 compatible with good status for phosphorus and average status for nitrogen (sub-cluster 4C,
 660 Figure 9), biological production of micro- and macroalgae would be lower, close to the
 661 average/fair threshold for phytoplankton. However, this functioning would result in significant

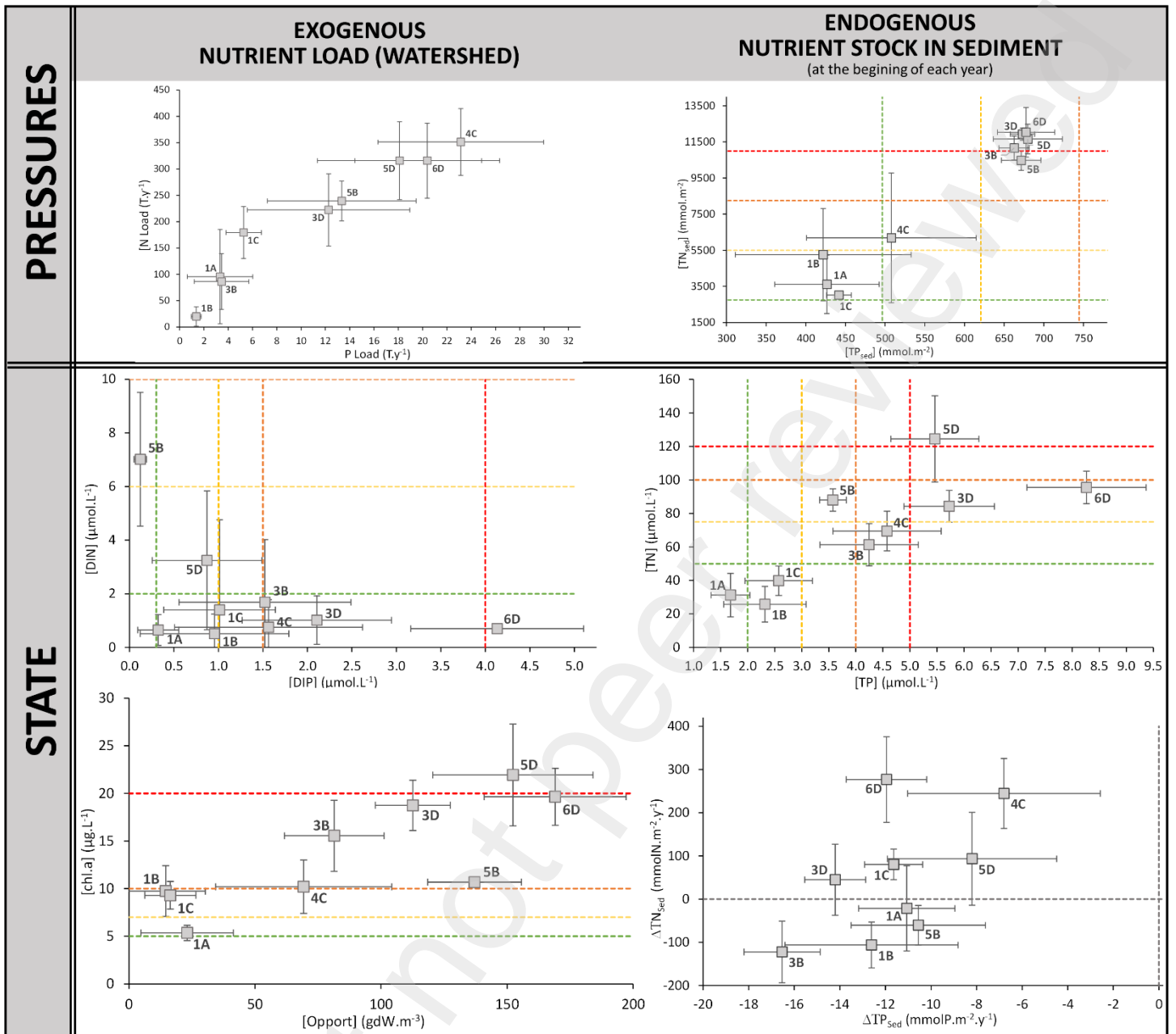
662 annual storage of nitrogen in the sediment compartment. 'Current' inputs would therefore be
663 likely to degrade a sediment compartment that was in good condition.

664 Even lower exogenous inputs (225 ± 64 Tonnes $N.y^{-1}$ and 12.5 ± 6.6 Tonnes $P.y^{-1}$) combined with
665 current sediment stocks (sub-clusters 3D and 5B) would still result in excessive biological
666 production. Depending on the competition between micro- and macroalgae, these inputs would
667 predominantly feed the 'Phytoplankton' (sub-cluster 3D) or 'Macrophyte' (sub-cluster 5B)
668 compartments and leave excess dissolved inorganic phosphorus (sub-cluster 3D) or dissolved
669 inorganic nitrogen (sub-clusters 5B) in the water column. Although such conditions of
670 exogenous and endogenous pressure are not compatible with the ecosystem's good ecological
671 status, they would make it possible to reverse the trend in terms of ecological trajectory by
672 favouring the removal of phosphorus in sediment and limiting the storage of nitrogen (sub-
673 cluster 3D) or even enabling its removal (sub-cluster 5B). An even more marked reduction in
674 inputs (86 ± 53 Tonnes $N.y^{-1}$ and 3.5 ± 2.3 Tonnes $P.y^{-1}$) associated with the current sediment
675 stock (sub-cluster 3B) would accentuate this trend towards the restoration of the sediment
676 compartment by favouring the massive destocking of nitrogen and phosphorous.

677 With exogenous inputs of the same order of magnitude (96 ± 90 Tonnes $N.y^{-1}$ and
678 3.3 ± 2.7 Tonnes $P.y^{-1}$) and a sediment compartment in good condition as regards nitrogen and
679 very good condition as regards phosphorus (sub-cluster 1A), the water column parameters and
680 phytoplankton biomass showed values compatible with good ecological status. The primary
681 production of micro- and macroalgae, jointly limited by nitrogen and phosphorus, did not leave
682 excess nutrients in the water column, and the sediment compartment tended to release nitrogen
683 and phosphorus. Such conditions reflect a balance between exogenous and endogenous fluxes.
684 Higher sediment stock associated with lower exogenous inflows (sub-cluster 1B) or,
685 conversely, lower sediment stock associated with higher exogenous inflows resulted in
686 phytoplankton production that was not compatible with good ecological status (chl.a close to

687 the average/fair threshold: Figure 9, 'State'). Thus, endogenous and exogenous conditions
688 corresponding to sediment stock in "good" condition for nitrogen and in "very good" condition
689 for phosphorus, and a reduction in exogenous inflows by a factor of 0.24 for nitrogen and 0.1
690 for phosphorus compared with current average annual inputs (402 Tonnes N.y⁻¹ and
691 31 Tonnes P.y⁻¹) would be compatible with the good ecological status of all the compartments
692 in the ecosystem. These conditions could be considered, based on what we know today, as a
693 target for admissible nutrient load for the Or Lagoon.

694



696 Figure 9: Pressure–state chart linking the state of the ecosystem ($[DIN]_{Lag}$ vs $[DIP]_{Lag}$; $[TN]_{Lag}$ vs $[TP]_{Lag}$; $[chl.a]_{Lag}$ vs $[Opport]_{Lag}$, the annual change in the sediment stock of nitrogen $[\Delta TN]_{sed}$ and phosphorus $[\Delta TP]_{sed}$ and the pressures exerted (from catchment and CRAS inputs and sediment stock) for the different sub-clusters. The horizontal and vertical lines correspond to the WFD thresholds.

701 4. Discussion

702 Since its creation in 2009, we have deliberately taken a pragmatic approach to continue to
 703 develop the GAME_{Lag} management tool. It initially provided a simple conceptualisation of the
 704 ecological functioning of an ecosystem; subsequently, its application at different sites during

705 the validation process revealed limitations in its use. This led to the choice of more realistic and
706 complex conceptualisations to attempt to overcome these limitations. As noted by Chapra et al.
707 (2003), the continuous improvement of management tools requires research into the scales at
708 which it is necessary and sufficient to describe the functioning of a complex system (Zwirn,
709 2006). Such an approach is dictated by the operational purpose of management support tools,
710 which must be capable of providing reliable answers to the questions posed by society within a
711 timeframe compatible with decision-making.

712 The simplicity of the GAMELag tool, linked to the fact that the hydrodynamic processes are
713 not resolved by the model but taken into account via adapted forcing conditions, makes it
714 possible to carry out a large number of simulations (six years simulated in less than 20 minutes
715 on a standard PC), which is essential for the analysis of exploratory scenarios.

716 *4.1. Relevance of the estimation method for admissible load*

717 Our findings show that exploratory scenario analysis carried out in two stages (clustering from
718 an AHC, which is then refined by taking into account ecological criteria) proves to be relevant
719 for describing change in coastal lagoons in response to pressures to which they are subjected,
720 as well as for defining the target for admissible nutrient load in these ecosystems. Considering
721 ecological criteria alone (conditions A to D in Table 5, without taking into account clusters 1
722 to 6) reveals only contrasting situations in which low exogenous flows are associated with
723 sediment stock in good condition (condition A) or in poor condition (condition B) or,
724 conversely, high exogenous flows are associated with sediment stock in poor condition
725 (conditions C and D). Yet transitional conditions in which trend reversals can occur – i.e. the
726 reduction in exogenous flows necessary to initiate the restoration of the sediment compartment
727 and thus reverse the ecological trajectory of the lagoon – is key information for environmental
728 managers. This information can confirm the relevance of measures to reduce exogenous inflows

729 even before WFD indicators highlight their positive impact (and consequently the investment
730 they require).

731 *4.2. Key compartments*

732 The model provides access to descriptors that may or may not be observable in situ and that
733 allow a detailed description of the simulated functioning of the system. Similarly, by allowing
734 processes to be decoupled, the model makes it possible to quantify the contribution of each
735 process in the overall functioning of the system. This revealed the key role played by
736 macroalgae and the sediment compartment in the functioning of the Or Lagoon.

737 *Macroalgae*

738 The succession of macroalgal and phytoplankton blooms is clearly shown in the model with the
739 assimilation of inorganic forms of nitrogen and phosphorus predominantly by macroalgae in
740 June and then by phytoplankton in July. This phytoplankton–macroalgal competition in June
741 could explain the late start of the summer phytoplankton blooms. Furthermore, the degradation
742 of opportunistic algae between April–May and July is the main source of DIP and could be the
743 cause of the excess phosphate in the water column simulated in the summer period. These
744 changes in the development of macroalgae thus appear to control both the start of the summer
745 plankton bloom and the phosphate concentration in the water column at that time.

746 In the absence of available data on the biomass of opportunistic algae present in the lagoon, few
747 parameters relevant to the conceptualisation of this compartment were included in the
748 estimation of the biogeochemical parameters of the model. New descriptors for this
749 compartment that link the biomass of opportunistic algae to the eutrophication status of a lagoon
750 (Fiandrino et al., 2022b) will now allow these to be used in global sensitivity analyses to
751 improve the calibration of parameters for this compartment.

752 A further limitation of the model is that it does not allow the estimation of the WFD
753 'Macrophyte' indicator based on the recovery rates of reference species. The current
754 conceptualisation of eelgrass beds in the GAMELag model does not include the assimilation of
755 nutrients by the root system, which may account for 50% of nitrogen assimilation (Hemminga
756 et al., 1991; Pedersen and Borum, 1992). Thus, in environmental conditions favourable to its
757 development, the growth of eelgrass would be strongly underestimated by the model. We
758 believe a new descriptor for the 'Macrophyte' compartment based solely on the biomass of
759 opportunistic algae is relevant on the assumption that a detailed understanding of changes in
760 seagrass is not necessary to determine admissible load. We consider that it is sufficient for the
761 model to be able to establish the links between the anthropic pressures exerted on the ecosystem
762 and the environmental conditions favourable to the development of eelgrass. The analysis of
763 simulated scenarios carried out in this study confirms this hypothesis.

764 The exogenous inputs of nitrogen and phosphorus that the Or Lagoon has received over several
765 decades have degraded this ecosystem, and the management measures put in place since the
766 beginning of the 2000s to reduce these inputs have not yet initiated a restoration dynamic. A
767 further reduction in inputs would have the direct consequence of limiting the production of
768 living matter in the water column (currently, mainly phytoplankton). Lastly, in conditions of
769 reduced phytoplankton production and therefore better light penetration in the water column,
770 nutrients from benthic flux could drive the production of opportunistic algae near the benthic
771 interface to the detriment of phytoplankton production. Such a shift from an ecosystem
772 dominated by phytoplankton to one dominated by opportunistic macroalgae has been described
773 in a lagoon close to the Or (the Méjean Lagoon) following measures aimed at reducing nutrient
774 inputs (Le Fur et al., 2019). This appears to be a first key step in the restoration of eutrophicated
775 lagoon environments. Then, in conditions in which the biomass of opportunistic macroalgae
776 and phytoplankton is compatible with 'good' ecological status, the restoration of the ecosystem

777 could continue with the natural recolonisation of the environment by perennial macrophytes
778 (Le Fur et al., 2019; De Wit et al., 2017).

779 *Sediment*

780 At present, the model cannot reproduce the change in sediment nitrogen stock over several
781 years. Variation in this stock results from the net balance between the sedimentation of
782 degraded organic matter and the release of ammonium resulting from the remineralisation of
783 this matter. Observations made in different Mediterranean lagoons (Ouisse et al., 2013; 2014)
784 show that the flux intensity of dissolved inorganic forms measured at the interface between the
785 benthic compartment and the water column varies primarily according to the season and the
786 quantity of nitrogen and phosphorus in the sediment (diffusive nutrient fluxes). These results
787 are consistent with data acquired in other Mediterranean lagoons (Chapelle et al., 1994; Le Fur,
788 2018; Zaaboub et al., 2014) and Australian lagoons (Eyre and Ferguson, 2002), and the order
789 of magnitude of DIN flux measured in lagoons with poor eutrophication status is in the order
790 of 5 – 8 mmol N.m⁻².d⁻¹. These values are higher than the simulated remineralisation rates in
791 the Or Lagoon, which vary between 0.4 (in winter) and 0.8 mmol N.m⁻².d⁻¹ (in summer). This
792 underestimation of the remineralisation of organic matter in sediment probably explains the
793 overestimation of nitrogen storage in the sediment.

794 The inability of the tool to carry out simulations over the medium to long term does not,
795 however, call into question its use in determining admissible load. The scenario analysis is
796 carried out on an annual scale (one element = one year) and is based on a complete set of
797 descriptors and the use of eight different parameterisations that allow changes in the
798 compartments from the ‘current’ situation to be correctly represented (with the exception of the
799 nitrogen stock in the sediment). Each parameterisation reflects specific simplifying assumptions
800 made during the conceptualisation stage and therefore has specific repercussions on the
801 simulation of ecosystem functioning. Taking these eight parameterisations into account leads

802 to eight possible simulations of ecosystem functioning that are compatible, in part, with the
803 observed reality.

804 Nonetheless, in order to allow simulations to be carried out over the medium to long term,
805 certain simplifying assumptions should be reassessed. At present, the sediment layer is assumed
806 to be oxic, but this assumption has not been verified, particularly during the summer period
807 when the thickness of the oxic sediment layer is very low (a few millimetres). Different models
808 of the nitrogen and phosphorus cycle in sediment take into account the oxygenation conditions
809 in a more or less realistic way (Chapelle, 1995; Plus et al., 2021). An early diagenesis module
810 that takes into account the oxygenation state of the sediment and the water column is currently
811 being developed in the GAMELag tool to account for anoxia phenomena in these coastal
812 lagoons used for shellfish farming (Le Ray et al., 2023).

813 *4.3. Collaboration between science and management*

814 Due to the limitations inherent in management tools discussed above, it is essential that their
815 development and deployment in given ecosystems be carried out within the framework of
816 projects that have been co-constructed, from their inception, by scientists and environmental
817 managers with shared objectives and interests. The application of the GAMELag model to the
818 Or Lagoon to address the problem of restoring this hypereutrophic environment has benefited
819 from such collaboration between scientists and managers, with substantial technical and
820 financial efforts made to acquire specific data and deploy adapted simulation tools.

821 This first experience using the GAMELag tool in operational conditions allowed us to review
822 the right level of balance between the scientific requirements linked to model development and
823 the operational expectations motivating this model. Given the constraints of developing a
824 ‘usable’ tool within an acceptable timeframe so that it can be ‘used’, choices were jointly made
825 and accepted by scientists and environmental managers, in particular by taking into account the

826 limitations of the tool by providing the uncertainties associated with the various descriptors in
827 the pressure–state chart. Its use has allowed recommendations to be made for supplementary
828 monitoring that could be carried out. In parallel with the measures planned in coming years to
829 reduce exogenous inputs, it will be important to monitor changes in sediment stocks of
830 nutrients. In addition to WFD monitoring, this data on sediment stocks would enable the lagoon
831 to be better positioned in the pressure–state chart in terms of internal pressures.

832 **5. Conclusion**

833 The current version of the GAMELag tool is the result of a long period of close collaboration
834 between lagoon managers, technical experts and scientists. Its application to various
835 Mediterranean lagoons, in particular the Or Lagoon, has confirmed its adaptability to sites with
836 complex functioning, and it is now available as a reference tool to assist managers of French
837 Mediterranean lagoons who want to adopt an admissible load approach.

838 With this approach, the GAMELag model is one key component in a global mission carried out
839 by lagoon managers with the support of scientific and technical experts. The improvements
840 currently being made to the tool should help make it possible to understand the time required
841 to restore eutrophicated lagoon ecosystems and to respond to issues involved in managing
842 environments and their uses (for example, shellfish farming) in a context of climate change.

843 **Funding and acknowledgements**

844 This research was carried out in the framework of several regional projects. The GAMELag
845 tool was funded by the oceanographic institute Ifremer and the Rhône-Mediterranean and
846 Corsica Water Agency (AERMC). The ORIGINS project received funding from Ifremer, the
847 Office of Geological and Mining Research (BRGM), the European Centre for Research and
848 Education in Environmental Geosciences (CEREGE) and the Syndicat Mixte du Bassin de l'Or
849 (SYMBO), which carried out the study on the functioning of the Or Lagoon with technical and
850 financial support from AERMC and scientific support from Ifremer.

851 The authors are extremely grateful to their colleagues from SYMBO: Ludovic Cases, for
852 hydrological data collection and management of the filmed monitoring network, and SYMBO
853 directors Jean-Marc Donnat and Flore Imbert-Suchet for their support. We would also like to
854 thank Grégory Messiaen, Elodie Foucault and Martine Fortuné from Ifremer for the nutrient
855 analyses. Cassandre Saguet (Ifremer) contributed to the development of the GAMELag tool,

856 and Olivier Banton and Sylvie St-Pierre (Hydriad Eau et Environnement) provided information
857 on inflows from the watershed. Elise Bradbury translated the article into English.

858 **CRedit author statement**

859 Annie Fiandrino: Conceptualization, Methodology, Software, Validation, Formal analysis,
860 Visualization, Writing - original draft, Writing - review & editing, Project administration,
861 Funding acquisition
862 Romain Pete: Methodology, Software, Writing - review & editing
863 Dominique Munaron: Data curation, Writing - review & editing, Project administration,
864 Funding acquisition
865 Pierre Théliér: Methodology, Visualization, Writing - review & editing, Project
866 administration, Funding acquisition,
867 Valérie Derolez: Data curation, Writing - review & editing
868 Lucille Picard: Software, Data curation, Validation, Formal analysis
869 Olivier Boutron: Conceptualization, Writing - review & editing
870 Columba Martinez-Espinosa C: Software, Writing - review & editing
871 Anaïs Giraud: Writing - review & editing, Funding acquisition
872 Stephane Stroffek: Writing - review & editing, Funding acquisition
873 Eve Le Pommelet: Methodology, Project administration, Funding acquisition
874 Vincent Ouisse: Conceptualization, Investigation, Data curation, Writing - review & editing

875 **References**

- 876 AERMC (2022). Estimer les flux de nutriments apportés aux lagunes méditerranéennes: une
877 étape clé pour définir une stratégie de maîtrise de leur eutrophisation. 37 p.
878 [https://www.eaurmc.fr/upload/docs/application/pdf/2022-](https://www.eaurmc.fr/upload/docs/application/pdf/2022-11/ok_sans_trait_coupe_081122__bat_impression_synthese_flux_lagunes_.pdf)
879 [11/ok_sans_trait_coupe_081122__bat_impression_synthese_flux_lagunes_.pdf](https://www.eaurmc.fr/upload/docs/application/pdf/2022-11/ok_sans_trait_coupe_081122__bat_impression_synthese_flux_lagunes_.pdf)
- 880 AERMC (2021). État des eaux lagunaires de Rhône-Méditerranée et de Corse. Bassin Rhône-
881 Méditerranée et de Corse. 135 p. + annexes (total 142 p.)
- 882 Borja, A., Dauer, D.M., Elliott, M., Simenstad, C.A. (2010). Medium- and long-term recovery
883 of estuarine and coastal ecosystems: patterns, rates and restoration effectiveness. *Estuaries and*
884 *Coasts*, vol.33, no.6, pp.1249–1260.
- 885 Castaings, J. (2012). Étude du fonctionnement hydrosédimentaire d'un écosystème lagunaire
886 sur des échelles de temps multiples: application au complexe étangs palavasiens - étang de l'Or
887 - canal du Rhône à Sète. <http://www.theses.fr>.
- 888 Chapelle, A., Mesnage, V., Mazouni, N., Deslous-Paoli, J.-M., Picot, B. (1994). Modélisation
889 des cycles de l'azote et du phosphore dans les sédiments d'une lagune soumise à une exploitation
890 conchylicole. *Oceanologica Acta*, 17(6), 609-620. Open Access version:
891 <https://archimer.ifremer.fr/doc/00039/15026/>
- 892 Chapelle, A. (1995). A preliminary model of nutrient cycling in sediments of a Mediterranean
893 lagoon. *Ecological Modelling*, 80(2-3), 131-147. [https://doi.org/10.1016/0304-3800\(94\)00073-](https://doi.org/10.1016/0304-3800(94)00073-Q)
894 [Q](https://doi.org/10.1016/0304-3800(94)00073-Q)
- 895 Chapra, S.C. (2003). Engineering Water Quality Models and TMDLs. *J. Water Resour. Plan.*
896 *Manage.* 129(4), 247-256.
- 897 Cloern, J. E., Schraga1, T. S., Nejad E., Martin C. (2020). Nutrient Status of San Francisco Bay
898 and Its Management Implications. *Estuaries and Coasts* (2020) 43:1299–1317
899 <https://doi.org/10.1007/s12237-020-00737-w>

900 Cloern, J.E. (2001). Our evolving conceptual model of the coastal eutrophication problem. *Mar*
901 *Ecol Prog Ser* 210:223-253

902 Colin, F., Crabit, A., Augas, J., Garnier, F., Favre, L., Lilti, V., Verlingue, U. (2017). Apports
903 d'eau aux lagunes côtières méditerranéennes - Propositions méthodologiques pour la
904 quantification des écoulements basées sur des mesures légères et des modèles synthétiques.
905 Rapport de fin de projet Agence de l'Eau RMC. Montpellier SupAgro (50 p).

906 Cugier, P., Thomas, Y., Bacher, C. (2022). Ecosystem modelling to assess the impact of rearing
907 density, environment variability and mortality on oyster production. *Aquaculture Environment*
908 *Interactions*, 14, 53-70. Publisher's official version: <https://doi.org/10.3354/aei00428>, Open
909 Access version: <https://archimer.ifremer.fr/doc/00766/87836/>

910 David, M. (2019). Influence des apports d'eaux souterraines sur le fonctionnement
911 hydrologique et biogéochimique des lagunes côtières méditerranéennes. Cas de la lagune de
912 l'Or / Influence of groundwater inputs on the hydrological and biogeochemical functioning of
913 coastal Mediterranean lagoons: case of Or lagoon. PhD Thesis, Université de Montpellier.

914 David, M., Bailly-Comte, V., Munaron, D., Fiandrino, A., Stieglitz, T. (2019). Groundwater
915 discharge to coastal streams – A significant pathway for nitrogen inputs to a hypertrophic
916 Mediterranean coastal lagoon. *Science of the Total Environment*, 677, 142-155. Publisher's
917 official version: <https://doi.org/10.1016/j.scitotenv.2019.04.233>, Open Access version:
918 <https://archimer.ifremer.fr/doc/00499/61095/>

919 Derolez, V., Bec, B., Cimiterra, N., Foucault, E., Messiaen, G., Fiandrino, A., Malet, N.,
920 Munaron, D., Serais, O., Connes, C., Gautier, E., Hatey, E., Giraud, A. (2021). OBSLAG 2020
921 - volet eutrophisation Lagunes méditerranéennes (période 2015-2020). Etat DCE de la colonne
922 d'eau et du phytoplancton, tendance et variabilité des indicateurs. RST/LER/LR/21.16.
923 <https://archimer.ifremer.fr/doc/00696/80768/>

924 Derolez, V., Bec, B., Munaron, D., Fiandrino, A., Pete, R., Simier, M., Souchu, P., Laugier, T.,
925 Aliaume, C., Malet, N. (2019). Recovery trajectories following the reduction of urban nutrient
926 inputs along the eutrophication gradient in French Mediterranean lagoons. *Ocean & Coastal*
927 *Management*, 171, 1-10.
928 Publisher's official version: <https://doi.org/10.1016/j.ocecoaman.2019.01.012>, Open Access
929 version: <https://archimer.ifremer.fr/doc/00478/58953/>

930 de Wit, R., Leruste, A., Le Fur, I., Sy, M.M., Bec, B., Ouisse, V., Derolez, V., Rey-Valette, H.
931 (2020) A Multidisciplinary Approach for Restoration Ecology of Shallow Coastal Lagoons, a
932 Case Study in South France. *Front. Ecol. Evol.* 8:108. doi: 10.3389/fevo.2020.00108

933 de Wit, R., Rey-Valette, H., Balavoine, J., Ouisse, V., Lifran, R. (2017). Ecological restoration
934 of coastal lagoons; prediction of ecological trajectories and economic valuation. *Aqua. Conserv.*
935 27, 137–157. doi: 10.1002/aqc.2601

936 Duarte, C.M., Conley, D.J., Carstensen, J., Sánchez-Camacho, M. (2009). Return to Neverland:
937 Shifting Baselines Affect Eutrophication Restoration Targets. *Estuaries and Coasts*, 32:29–36
938 DOI 10.1007/s12237-008-9111-2

939 Elliott, M., Burdon, D., Hemingway, K.L., & Apitz, S.E. (2007). Estuarine, coastal and marine
940 ecosystem restoration: Confusing management and science - A revision of concepts. *Estuarine,*
941 *Coastal and Shelf Science*, 74(3), 349–366. <http://doi.org/10.1016/j.ecss.2007.05.034>

942 Eyre, B., Ferguson, A., Webb, A., Maher, D., Oakes, J. (2011). Denitrification, n-fixation and
943 nitrogen and phosphorus fluxes in different benthic habitats and their contribution to the

944 nitrogen and phosphorus budgets of a shallow oligotrophic sub-tropical coastal system
945 (southern Moreton Bay, Australia). *Biogeochemistry*, 102 (1), 111–133.

946 Eyre, B.D., Ferguson, A.J.P. (2002). Comparison of carbon production and decomposition,
947 benthic nutrient fluxes and denitrification in seagrass, phytoplankton, benthic microalgae- and
948 macroalgae-dominated warm/temperate Australian lagoons. *Mar Ecol Prog Ser* 229, 43-59.

949 Ferrarin, C., Umgiesser, G., Bajo, M., Bellafiore, D., De Pascalis, F., Ghezzi, M., Mattassi, G.,
950 Scroccaro, I. (2010). Hydraulic zonation of the lagoons of Marano and Grado, Italy. A
951 modelling approach. *Estuar. Coast. Shelf Sci.* 87 (4):561–572 [http://doi.org/10.1016/
952 j.ecss.2010.02.012](http://doi.org/10.1016/j.ecss.2010.02.012).

953 Fiandrino, A., Pete, R., Giraud, A., Picard, L., Stroffek, S. (2022a). Le modèle GAMELag pour
954 l'étude du fonctionnement des écosystèmes lagunaires méditerranéens: synthèse des
955 caractéristiques techniques et utilisation. ODE/UL/LER/LR/22.15.
956 <https://archimer.ifremer.fr/doc/00803/91518/>

957 Fiandrino, A., Cimiterra N., Giraud, A., Stroffek, S. (2022b). Vers un descripteur du
958 compartiment « Macrophyte » pour le modèle GAMELag. Note basée sur l'analyse de la base
959 de données « Macrophyte – RSL ». ODE/UL/LER/LR/22.16.
960 <https://archimer.ifremer.fr/doc/00806/91753/>

961 Fiandrino, A., Ouisse, V., Dumas, F., Lagarde, F., Pete, R., Malet, N., Le Noc, S., de Wit, R.
962 (2017). Spatial patterns in coastal lagoons related to the hydrodynamics of seawater intrusion.
963 *Mar. Pollut. Bull.* 119, 132–144. <https://doi.org/10.1016/j.marpolbul.2017.03.006>.

964 Greening, H., Janicki, A., Sherwoo, E.T., Pribble, R., Johansson, J.O.R. (2014). Ecosystem
965 responses to long-term nutrient management in an urban estuary: Tampa Bay, Florida, USA.
966 *Estuarine, Coastal and Shelf Science* 151 (2014) A1-A16.
967 <http://dx.doi.org/10.1016/j.ecss.2014.10.003>.

968 Gordon, J.R., D.C., Boudreau, P.R., Mann, K.H., Ong, J.-E., Silvert, W.L., Smith, S.V.,
969 Wattayakorn, G., Wulff, F., Yanagi, T. (1996). LOICZ biogeochemical modelling guidelines.
970 LOICZ/R&S/95-5, VI +96 pp. LOICZ, Texel, The Netherlands.

971 Hemminga, M.A., Harrison, P.G., van Lent, F. (1991). The balance of nutrient losses and gains
972 in seagrass meadows. *Marine Ecology Progress Series*, 71:85-96.

973 Hydriad (2022). Calculs de flux polluants sur les tributaires des lagunes du bassin Rhône
974 Méditerranée.
975 [https://www.eaurmc.fr/upload/docs/application/pdf/202207/hydriad_flux_lagunes_juin_2022.
976 pdf](https://www.eaurmc.fr/upload/docs/application/pdf/202207/hydriad_flux_lagunes_juin_2022.pdf)

977 Ifremer (2011). Réseau de Suivi Lagunaire du Languedoc-Roussillon: Bilan des résultats 2010.
978 RST/LER/LR11.01. <https://archimer.ifremer.fr/doc/00118/22918/>

979 Ifremer (2003). Réseau de Suivi Lagunaire du Languedoc-Roussillon: Bilan des résultats 2002.
980 Rapport RSL-03/2003, 523 p. <https://archimer.ifremer.fr/doc/00419/53085/>

981 Le Fur, I., de Wit, R., Plus, M., Oheix, J., Derolez, V., Simier, M., Malet, N., Ouisse, V. (2019).
982 Re-oligotrophication trajectories of macrophyte assemblages in Mediterranean coastal lagoons
983 based on 17-year time-series. *Marine Ecology Progress Series*, 608, 13-32.
984 Publisher's official version: <https://doi.org/10.3354/meps12814>, Open Access version:
985 <https://archimer.ifremer.fr/doc/00474/58555/>.

986 Le Fur, I. (2018). Rôle des macrophytes dans la restauration des milieux lagunaires: successions
987 écologiques / Role of macrophytes in the restoration of lagoon environments: ecological
988 succession. PhD Thesis, Université de Montpellier.

- 989 <https://archimer.ifremer.fr/doc/00498/60959/>
- 990 Le Fur, I., de Wit, R., Plus, M., Oheix, J., Simier, M., Ouisse, V. (2018). Submerged benthic
991 macrophytes in Mediterranean lagoons: distribution patterns in relation to water chemistry and
992 depth. *Hydrobiologia*, 808(1), 175-200. <https://doi.org/10.1007/s10750-017-3421-y>.
- 993 Le Ray, J., Bec, B., Fiandrino, A., Lagarde, F., Cimiterra, N., Raimbault, P., Roques, C.,
994 Rigaud, S., Régis, J., Mostajir, B., Mas, S., Richard, M. (2023). Impact of anoxia and oyster
995 mortality on nutrient and microbial planktonic components: A mesocosm study. In press in
996 *Aquaculture* 556.
- 997 Mongrue, R., Vanhoutte-Brunier, A., Fiandrino, A., Valette, F., Ballé-Béganton, J., Pérez
998 Agúndez, J.A., Gallai, N., Derolez, V., Roussel, S., Lample, M., Laugier, T. (2013). Why, how,
999 and how far should microbiological contamination in a coastal zone be mitigated? An
1000 application of the systems approach to the Thau lagoon (France). *Journal of Environmental*
1001 *Management*, 118, 55–71. <http://doi.org/10.1016/j.jenvman.2012.12.038>
- 1002 Morris, M. (1991). Factorial sampling plans for preliminary computational dynamics.
1003 *Technometrics* 33, 161–174
- 1004 MTES, 2018. Ministère de la Transition Ecologique et Solidaire, MTES (2018). Guide relatif
1005 aux règles d'évaluation de l'état des eaux littorales dans le cadre de la DCE. 277 p.
1006 <https://professionnels.afbiodiversite.fr/sites/default/files/pdf/estuaires/GuideREEEL-DCE-MT>
1007 [ES2018.pdf](https://professionnels.afbiodiversite.fr/sites/default/files/pdf/estuaires/GuideREEEL-DCE-MT)
- 1008 Newton, A., Cañedo-Argüelles, M., March, D., Goela, P., Cristina, S., Marta Zacarias, M.,
1009 Icely, J. (2022). Assessing the effectiveness of management measures in the Ria Formosa
1010 coastal lagoon, Portugal. *Front. Ecol. Evol.* 10:508218. doi: 10.3389/fevo.2022.508218
- 1011 Ouisse, V., Fiandrino, A., Giraud, A. (2020). EXpertise sur les stocks SEDimentaires en milieu
1012 lagunairE. Rapport du Projet EXSEDE. R.ODE/UL/LER/LR 20.13.
1013 <https://doi.org/10.13155/75435>
- 1014 Ouisse, V., Fiandrino, A., de Wit, R., Giraud, A., Malet, N. (2014). DEvenir du Phosphore et
1015 de l'Azote dans un contexte de ResTauratIon des milieux lagunaires méditerranéens -
1016 DEPART. R.INT.ODE/UL/LER-LR 2014-14-22
- 1017 Ouisse, V., Fiandrino, A., de Wit, R., Malet, N. (2013). Restauration des écosystèmes
1018 lagunaires: évaluation du rôle du sédiment et des herbiers à phanérogames. *RST/LERLR* 13-
1019 09. <https://archimer.ifremer.fr/doc/00166/27774/>
- 1020 Pedersen, M.F., Borum, J. (1992). Nitrogen dynamics of eelgrass *Zostera manna* during late
1021 summer period of high growth and low nutrient availability. *Marine Ecology Progress Series*
1022 8055-733.
- 1023 Pérez-Ruzafa, A., Pérez-Ruzafa, I.M., Newton, A., Marcos, C. (2019). Chapter 15. Coastal
1024 Lagoons: Environmental variability, ecosystem complexity, and goods and services uniformity
1025 in coast and estuaries, the future. Eds E. Wolanski, J. Day, M. Elliott, R. Ramachandran, 730.
1026 Amsterdam: Elsevier. doi: 10.1016/B978-0-12-814003-1.00015-0
- 1027 Pete, R., Guyondet, T., Bec, B., Derolez, V., Cesmat, L., Lagarde, F., Pouvreau, S., Fiandrino,
1028 A., Richard, M. (2020a). A box-model of carrying capacity of the Thau lagoon in the context
1029 of ecological status regulations and sustainable shellfish cultures. *Ecological Modelling*, 426,
1030 109049 (17p.). Publisher's official version: <https://doi.org/10.1016/j.ecolmodel.2020.109049>,
1031 Open Access version: <https://archimer.ifremer.fr/doc/00622/73395/>.

- 1032 Pete, R., Fiandrino, A., Malet, N. (2020b) : Fonctionnement écosystémique de la lagune de
 1033 Biguglia. Partie 2 : Déploiement du modèle écosystémique GAMELag sur la lagune de
 1034 Biguglia. 31p. ODE/UL/LER-PAC/20.01. <https://archimer.ifremer.fr/doc/00604/71564/>
- 1035 Pete, R., Fiandrino, A., Mahevas, S., Plus, M., & de Wit, R. (2017). Fiabilisation de l’outil
 1036 GAMELag. Rapport final du Contrat n°2015 0346. RST.ODE/UL/LER-LR 17-12.
- 1037 Picard, L. (2021). Etude du devenir des nutriments dans l’étang de l’Or: application du modèle
 1038 GAMELag sur l’étang de l’Or. Rapport d’étude final.
- 1039 Plus, M., Thouvenin, B., Andrieux, F., Dufois, F., Ratmaya, W., Souchu, P. (2021). Diagnostic
 1040 étendu de l’eutrophisation (DIETE). Modélisation biogéochimique de la zone Vilaine-Loire
 1041 avec prise en compte des processus sédimentaires. Description du modèle Bloom
 1042 (Biogeochemical Coastal Ocean Model). RST/LER/MPL/21.15.
 1043 <https://archimer.ifremer.fr/doc/00754/86567/>
- 1044 Saguet, C., Pete, R., Massinelli, L., Ouisse, V., Mahévas, S., Derolez, V., Giraud, A., Stroffek,
 1045 S., Fiandrino, A. (2019). GAMELag: de l’optimisation de l’outil à « l’exploration » des Flux
 1046 Maximaux Admissibles. Rapport Final du Contrat n°2018 0158.
- 1047 Saltelli, A., Tarantola, S., Campolongo, F. (2000). Sensitivity Analysis as an Ingredient of
 1048 Modeling. *Institute of Mathematical Statistics*, 15(4), 377–395.
 1049 <http://www.jstor.org/stable/2676831>
- 1050 SDAGE (2022). SDAGE Rhône Méditerranée: [https://rhone-mediterranee.eaufrance.fr/](https://rhone-mediterranee.eaufrance.fr/gestion-de-leau/sdage-2022-2027-en-vigueur)
 1051 [gestion-de-leau/sdage-2022-2027-en-vigueur](https://rhone-mediterranee.eaufrance.fr/gestion-de-leau/sdage-2022-2027-en-vigueur); SDAGE Corse: [https://corse.eaufrance.fr/](https://corse.eaufrance.fr/gestion-de-leau/dce-sdage)
 1052 [gestion-de-leau/dce-sdage](https://corse.eaufrance.fr/gestion-de-leau/dce-sdage).
- 1053 SDAGE (2018). Définir les flux admissibles pour gérer les bassins versants fragiles vis-à-vis
 1054 des phénomènes d’eutrophisation – Bassin Rhône Méditerranée
- 1055 SYMBO (2019). Fonctionnement hydrodynamique de l’étang de l’Or – Bilan imports/exports
 1056 et hiérarchisation des sources de matière. Rapport d’étude final.
- 1057 SYMBO and Acteon, (2021). Etude bilan du Contrat de Bassin Versant de l’étang de l’Or.
 1058 Rapport de phase 1. Bilan technico-financier et environnemental des actions engagées, 126 p.
- 1059 Sridharan, V.K., Quinn, N.W.T., Kumar, S., McCutcheon, S.C., Ahmadisharaf, E., Fang, X.,
 1060 Zhang, H.X., Parker, A. (2021). Selecting Reliable Models for Total Maximum Daily Load
 1061 Development: Holistic Protocol. *J. Hydrol. Eng.*, 26(10): 04021031.
- 1062 Umgiesser, G., Ferrarin, C., Cucco, A., De Pascalis, F., Bellafiore, D., Ghezzi, M., Bajo, M.,
 1063 (2014). Comparative hydrodynamics of 10 Mediterranean lagoons by means of numerical
 1064 modeling. *J. Geophys. Res.* 119:2212–2226 <http://doi.org/10.1002/2013JC009512>.
- 1065 Vijay, A., Munnooru, K., Reghu, G., Gera, A., Vinjamuri, R., Ramanamurthy, M.V. (2021).
 1066 Nutrient dynamics and budgeting in a semi-enclosed coastal hypersaline lagoon. *Environmental*
 1067 *Science and Pollution Research*. <https://doi.org/10.1007/s11356-021-15334-y>
- 1068 Voulvoulis, N., Arpon, K.D., and Giakoumis, T. (2017). The EU Water Framework Directive:
 1069 from great expectations to problems with implementation. *Sci. Total Environ.* 575, 358–366.
 1070 doi: 10.1016/j.scitotenv.2016.09.228
- 1071 Willmott, C.J., Robeson, S.M., Matsuura, K. (2012). A refined index of model performance.
 1072 *Int. J. Climatol.* 32 (13): 2088–2094 <http://doi.org/10.1002/joc.2419>.
- 1073 Zaaboub, N., Ounis, A., Hellali, M.A., Béjaoui, B., Libelo, A., Dasilva, E., Aleya, L. (2014).
 1074 Phosphorus speciation in southwestern Mediterranean lagoon sediments (North Tunisia). *Ecol.*
 1075 *Eng.* 73, 115–125.

- 1076 Zaldívar, J.-M., Cardoso, A.C., Viaroli, P., Newton, A., De Wit, R., Ibañez, C., Reizopoulou,
1077 S., Somma, F., Razinkovas, A., Basset, A., Marianne Holmer, M., Murray, N. (2008).
1078 Eutrophication in transitional waters: an overview. *Trans. Waters Monogr.* 2, 1–78.
1079 DOI 10.1285/i18252273v2n1p1
- 1080 Zwirn, H.P. (2006). *Les systèmes complexes. Mathématiques et biologie* (Odile Jacob).